www.directivepublications.org

Journal of Applied Sciences

ISSN 2998-9159

Research Article

Polymer Electrolyte for Solar Cell.

Nujud Badawi[1] and M. Bhuyan[2].

[1] *University of Hafr Al–Batin College of Science, Hafer Al-Batin 39921, Saudi Arabia.*
[2] *Institute of Physics, Sachivalaya Marg, Bhubaneswar 751 005, Odisha, India.*

Abstract

There have been reviews of high-performance polymer electrolytes for dye-sensitised solar cell applications. Recent developments in dye-sensitised solar cell (DSSC) technology have shown that adding inorganic nanofillers to polymer electrolytes is a viable way to improve the devices' electrochemical performance and structural stability. We describe our developed systems and stacks for polymer electrolyte membrane (PEM) electrolysis that are optimised for direct coupling to a photovoltaic (PV) panel. An effective substitute for liquid electrolytes is provided by gel polymer electrolytes (GPEs). They have higher interfacial adhesion qualities and similar conductivity. Additionally, GPE can lessen the leakage problem because the salt that has been dissolved in the solvent is contained inside the polymer network. Analysing charge-transfer mechanisms in the electrolyte's bulk and at its contacts with other materials is crucial because it plays a significant part in the current generation process in dye-sensitised solar cells (DSSCs). Gel polymer electrolytes are more useful and convenient to use than liquid electrolytes due to solvent confinement; however, further research is still required to maximise their efficacy.

Keywords : Polymer Electrolyte; Solar Cell; Gel Polymer; Dye-sensitised Solar Cell.

INTRODUCTION

Buildings are responsible for 26% of global energy-related carbon emissions and 30% of global final energy consumption, according to the International Energy Agency. Climate change mitigation requires zero-carbon-ready buildings, which frequently use renewable energy. One of the most widely available green energy sources for urban structures is solar energy. However, aesthetic concerns and rooftop space constraints limit the development of retrofit rooftop solar panels. A solution that smoothly incorporates solar power generation into a building's structure, including windows and facades, is called building-integrated photovoltaics, or BIPVs. This strategy achieves efficient land-use and architectural aesthetics while enabling power generation [Shukla, A. K., Sudhakar, K., & Baredar, P. (2017)]. Semi-transparent photovoltaics (STPVs) have attracted a lot of attention due to the growing use of windows or semi-transparent envelopes as key architectural features in modern structures, such as upscale apartment complexes and shopping centres.

It is possible to integrate electricity generation with other building material functions by installing solar photovoltaic installations on the building skin [Enkvist, P., Dinkel, J., Company, C. L.-M. &, & 2010] [Nujud et al, 2024]. Since PV integration in building facades represents a significant advancement in urban solar PV applications, more and more countries have set goals for using solar PV in the building sector in response to the benefits of building integration [G. L.-R. and S. E., & 2015]. In addition to reducing traditional energy consumption, the solar PV system also reduces emissions from diesel generators and peak electricity production from coal and oil [Li, G. 2013]. These days, energy efficiency is a key factor in deciding whether to use PV in buildings [Li et al., 2013]. Even though PV is currently up to five times more expensive than grid power, it is generally anticipated that it will be able to significantly contribute to mainstream power production in the coming century [Li, 2014]. One of the sophisticated technologies for the effective use of solar power is solar photovoltaics [Li, 2012]. Future solar photovoltaic applications must take into account four key factors: cost reduction, storage system, BIPV applications, and efficiency improvement [Peng, 2011]. Buildings that use BIPV products become energy producers instead of consumers. For improved performance in this development,

***Corresponding Author:** **Mrutunjaya Bhuyan,** Institute of Physics, Sachivalaya Marg, Bhubaneswar 751 005, Odisha, India. **Email:** mrutunjaya.b@iopb.res.in.
Received: 10-July-2025, Manuscript No. JOAS - 4978 **; Editor Assigned:** 11-July-2025 **; Reviewed:** 28-August-2025, QC No. JOAS - 4978 **;**
Published: 01-September-2025, **DOI:** 10.52338/joas.2025.4978.
Citation: **Mrutunjaya Bhuyan.** Polymer Electrolyte for Solar Cell. Journal of Applied Sciences. 2025 September; 13(1). doi: 10.52338/joas.2025.4978.
Copyright © 2025 **Mrutunjaya Bhuyan.** This is an open access article distributed under the Creative Commons Attribution License, which permits unrestricted use, distribution, and reproduction in any medium, provided the original work is properly cited.

product technology must be combined with BIPV technology [Held, M., & Ilg, R. (2011)].

Gel polymer electrolytes (GPEs) are a game-changing technology for electric vehicle advancement because of their enormous potential to advance high-energy density. Numerous GPEs have been developed based on various materials, such as hybrid solid-state batteries, dendritic-free polymer gel electrolytes, flame-retardant GPEs, and 3D printed GPEs. Considerable attention has also been paid to enhancing the interaction between electrodes and GPEs. With increased efficiency and dependability, the incorporation of gel-based electrolytes into solid-state electrochemical devices holds the potential to completely transform energy storage technologies. These developments are used in many different industries, but they are especially useful in renewable energy and electric cars.

Due to their scientific significance in the field of energy conversion, dye-sensitised solar cells (DSSCs) have attracted a lot of attention in the past 20 years. At the moment, DSSC uses natural dyes, quantum-dot sensitisers, perovskite-based sensitisers, metal-free organic dyes, and inorganic ruthenium (Ru)-based sensitisers. Due to their low cost, ease of preparation, easy attainability, and environmental friendliness, metal-free, quantum-dot sensitiser, perovskite-based sensitiser, and natural dyes have emerged as a competitive alternative to costly and scarce Ru-based dyes. Because of their instability, negative dye aggregation, and narrow absorption bands ($\Delta\lambda \approx 100–250$ nm), the majority of Ru-based dye substitutes have so far proven to be less effective than Ru-based dyes [Shalini and others, 2016]. Dye-sensitised solar cells (DSSCs) promote the development of photovoltaic devices with high conversion efficiency at low cost in a system that converts pure and non-conventional solar energy to electricity. When assessing the performance of DSSCs, the dye's function as a sensitizer is crucial. Due to their extreme availability, affordability, and biodegradability, natural dyes, also known as organic dyes, have emerged as a viable alternative to the costly and scarce inorganic sensitisers. Over the years, various plant parts, including fruits, leaves, flowers, petals, and bark, have been tested as sensitisers. The characteristics of these pigments, along with a few other factors, lead to an improvement in the DSSCs' operating standard [Adedokun, O., Titilope, K., & Awodugba, A. O. (2016)]. According to the study, strategically adding graphene, which can be synthesised at a reasonable cost, to specific photoanode layers can significantly increase the power conversion efficiency of DSSCs.

One promising new low-cost thin-film technology is the organic solar cell (OSC). The advancement of low bandgap organic materials synthesis and device processing technology has allowed OSCs to surpass single junction solar cells' 16% power conversion efficiency (PCE) and organic–organic tandem solar cells' 17% PCE. The primary obstacle to the commercial application of OSCs is the devices' low stability. In recent decades, the development of sustainable and renewable energy has gained popularity as the world's energy needs continue to rise. With their low cost, lightweight, flexible, semitransparent, and simple fabrication, organic solar cells (OSCs) have become a promising renewable energy technology. [Zhang, J., Guo, X., Facchetti, A., Tan, H. S., & Yan, H. (2018)]Numerous studies conducted in recent years have concentrated on increasing the power conversion efficiency (PCE) of OSCs through the use of techniques like the design of high-performance donor and acceptor materials, the use of ternary active layers, tandem device structures, carrier transport layer optimization, and fabrication process optimization.

Novel polymer blends with improved properties over conventional plastics and demonstrated costeffective advantages over the synthesis of new polymers were developed as a result of the recent interest in multifunctional materials with customizable performances. However, most polymer blends are immiscible, so to create an alloy with appropriate performance, proper compatibilisation is required. A new method based on inserting micro- and nanostructured inorganic fillers into polymer blends has recently surfaced in addition to the conventional compatibilisation techniques (such as reactive compatibilisation and the addition of graft or branched copolymers) [Dorigato, A., & Fredi, G. (2024)]. A viable substitute that might provide solar power at a significantly lower cost than other, more traditional inorganic photovoltaic technologies is organic solar cells, both in the hybrid dyesensitised technology and in the full organic polymeric technology. a life cycle analysis of a typical bulk heterojunction organic solar cell produced in a lab and contrasts the results with those of other photovoltaic technologies produced in an industrial setting. In addition, a thorough material inventory from raw materials to the finished photovoltaic module is provided, which enables us to spot possible supply chain bottlenecks for a major industrial output in the future. The energy payback time and CO_2 emission factor for the organic photovoltaic technology are comparable to those of other inorganic photovoltaic technologies, even at this early stage of laboratory production. This shows that there is still much space for improvement if the fabrication process is optimised and scaled up to an industrial process [García-Valverde, R., Cherni, J. A., & Urbina, A. (2010)].

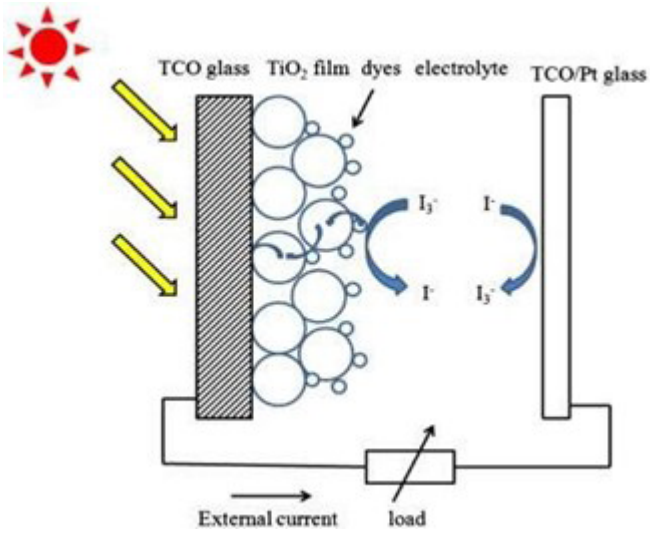
Over the past few decades, bulk heterojunction (BHJ) organic solar cells (OSCs) have garnered a lot of interest in the photovoltaics industry due to their remarkable bendable, wearable, and portable qualities as well as their potential for large-scale production [Mehboob, et al (2021)]. Furthermore, its optical bandgap, energy levels, charge transport mobility, and other physical characteristics can be tailored for the

perfect target devices because organic materials can undoubtedly undergo a variety of molecular modifications [Luo et al., 2022]. Semi-transparent organic solar cells (ST-OSCs), one of the many varieties of OSCs, are the focus of practical research areas like power generation when mounted on windows, buildings, cars, and greenhouse exterior walls.

DYE-SENSITISED SOLAR CELLS

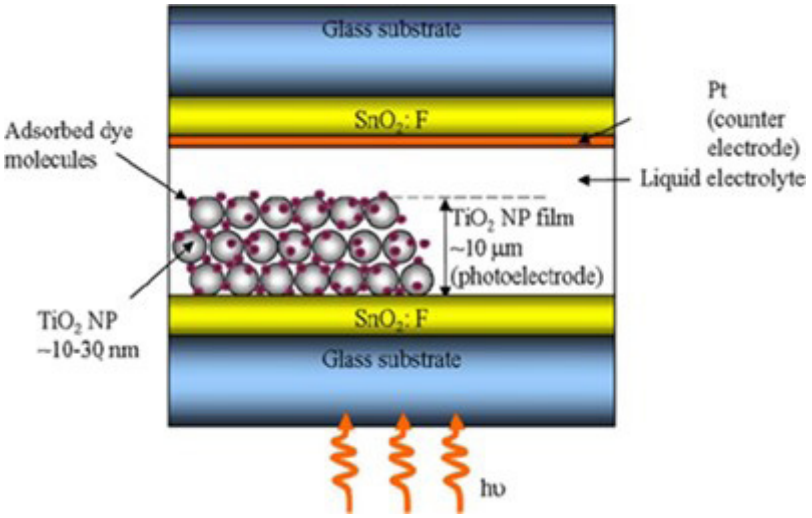
A semiconductor photovoltaic device called a dye-sensitised solar cell (DSSC) directly transforms solar radiation into electrical current. The DSSC's working principle is depicted in **Figure 1** [Liang, J., Sumathy, K., & Gong, J. (2012)]. An electron is injected into the mesoporous oxide film's conduction band when the dye sensitiser is excited by sunlight. Before being gathered by the electrolyte at the cathode surface to finish the cycle, these electrons diffuse to the anode and are used at the external load. Safe energy supplies are essential to human society's prosperity, and fossil fuels have long been the most dependable energy source. But since fossil fuels are a nonrenewable energy source, their depletion is both inevitable and imminent in this century. Renewable energy, particularly solar energy, has garnered a lot of attention as a solution to this issue because it directly transforms solar radiation into electrical power without affecting the environment. Different photovoltaic devices, such as hybrid, inorganic, and organic solar cells, were manufactured one after the other in the past. Even though silicon-based solar cells have a high conversion rate, their use is limited to astronautic and aeronautic technology due to their expensive modules and difficult manufacturing process. Because of their easy fabrication and intrinsic low module cost, organic solar cells have been the focus of research for both residential and commercial applications. Furthermore, organic solar cells are more flexible and lightweight than traditional silicon-based crystalline solar cells. Dye-sensitised solar cells (DSSCs) are the most effective and straightforward technology among all organic solar cells. This study looks at the novel technology's operation, current state of development, and prospects for the future.

Figure 1. Diagram of the dye-sensitised solar cell schematic [Gong, J., Liang, J., & Sumathy, K. (2012)].



The glass substrate, transparent conducting layer, TiO_2 nanoparticles, dyes, electrolyte (I-/I3 or Co II/Co III complexes), and counter electrode (Carbon or Pt) covered with a sealing gasket are among the various layers of components used in the current DSSC construction. **Figure .2** depicts the standard DSSC construction [Michal Sokolský and Július Cirák 2010]. The primary components of dye-sensitised solar cells are conducting substrates, semiconductor films, nonporous dye sensitisers, redox electrolytes, and counter electrodes. [Fan-et al., 2007] [Andualem, A., & Demiss, S. (2018)]. The future of DSSC in the field of photovoltaic cells appears to be extremely bright. Grätzel cells, another name for DSSCs, are a novel kind of solar cell that has garnered a lot of attention because of their low manufacturing costs and environmental friendliness. A counter electrode, an electrolyte with iodide and triiodide ions, and an electrodeabsorbed dye made of nanocrystalline porous semiconductors make up a DSSC. In DSSCs, the dye that serves as a sensitiser is crucial to the absorption and electrical conversion of incident light rays. Because the dyes absorb a portion of the visible light spectrum, they produce photosensitization on wide band-gap mesoporous metal oxide semiconductors, which is the basis for DSSC operations. In addition to its significant environmental benefits, the utilisation of natural pigments as sensitising dye for solar energy conversion is noteworthy for its ability to improve economics. Large dye collections, including natural dyes, can be used as light-harvesting elements to provide the charge carriers, making DSSCs more intriguing [Adedokun, O., Titilope, K., & Awodugba, A. O. (2016)].

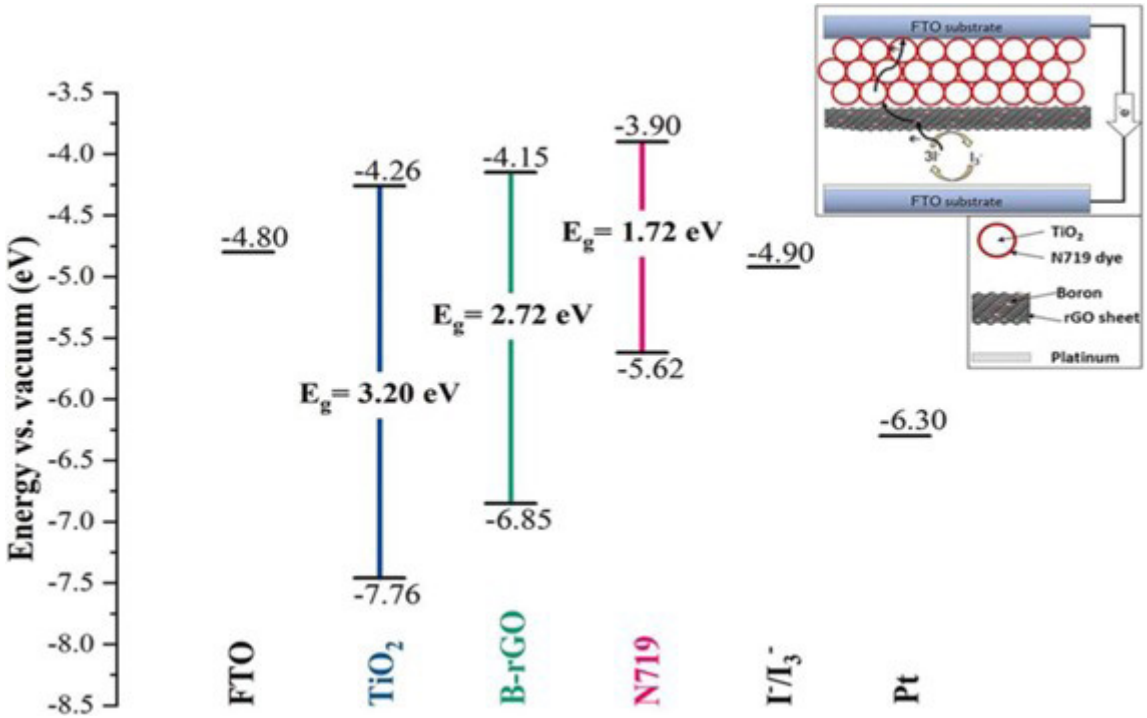
Figure 2. Typical design of a dyesensitized solar cell. [Michal Sokolský and Július Cirák 2010].



With a multilayer structure to enhance light absorption and electron collection efficiency, carbon dioxide replacing TiO_2 as the electron acceptor, oxygen as the electron donor and oxidation product, and dye replacing chlorophyll as the light-harvesting element for the production of excited electrons, DSSC functions similarly to photosynthesis. The DSSC's light-driven electrochemical process is regenerative, and the working voltage it generates is equal to the difference between the mediator's redox potential and the chemical potential of the TiO_2 (Fermi level). At the cathode, electrons are transferred to the electrolyte. The I −/I3 − electrolytes act as intermediaries between the TiO_2 photo electrode and the cathode, which is a carbon-plated counter electrode. The iodide molecules are oxidised into tri-iodide ions (I3 −) as a result of the oxidised dye receiving an electron from the I-ion redox to replace the lost electron. Equation 4 describes this process. As a result, the Ru compound-sensitised DSSC efficiency adsorbed on semiconductor nano-crystalline TiO_2 has increased to 11–12% [Y. et al. (2006) [R. and others, 2008]. The major contributor to efficiency losses in DSSCs is when electrons recom one major obstacle to DSSCs' high efficiency is electron recombination. This process occurs at the TiO_2/ electrolyte interface when an electron that was injected from the excited dye molecule into the conduction band of the TiO_2 photoanode recombines with an electron vacancy in the electrolyte. The device's overall efficiency is ultimately limited by this recombination, which lowers the number of electrons available to contribute to the current generation within the device [Research, A. T.-C. A. E., & 2022]. At the TiO2/electrolyte interface, bind directly with electrolyte holes. Doping [Wang, D., Zou, W., Chen, Y., & Duan, J. (2023)], surface modification [Mahalingam, S., Manap, A., Rabeya, R., ... K. L.-E., & 2023], and the use of alternative electrolytes [Sayah, D., & T. G.-A. S. C., & 2024] are some of the methods used to suppress recombination (TiO_2/electrolyte) and increase DSSC efficiency. The basic workings of photoanode-based dye-sensitised solar cells (DSSC) are still unclear. Because of the behavioural changes in charge transport, the modification of the photoanodes has an impact on the overall performance of the DSSC.[Mahalingam et al. 2025] fabricate a boronreduced graphene oxide (B-rGO) series with varying numbers of photoanodes by controlling the concentrations of the precursors. In comparison to both lower and higher B-rGO concentrations, the DSSC with 0.2 weight percent B-rGO shows the highest efficiency and EQE. The 0.2 weight percent B-rGO DSSC exhibits the lowest charge transfer resistance according to electrochemical impedance spectroscopy, indicating inhibited recombination processes. But even at low B-rGO levels, the trend in electron lifetime that has been observed—longest for the reference DSSC and decreasing with B-rGO concentration—indicates the possibility of electron trapping sites. Effective electron transfer from the excited dye to the TiO_2 conduction band is made possible by the ideal B-rGO concentration (0.2 wt%), which may improve light scattering or reduce recombination. Effective collection of generated charges prior to recombination is another prerequisite for efficient light conversion. Better charge transport characteristics within the device may be indicated by the higher EQE in B-rGO (0.2), which is a result of B-rGO. Although B-rGO has potential advantages, the lower EQE and efficiency of the B-rGO (0.3) indicate that using a very thick B-rGO layer may have disadvantages. Light may be trapped inside the device rather than reaching the collecting electrode due to excessive light scattering caused by an excessively thick B-rGO layer. More recombination centres could be introduced into the device by a thick BrGO layer, which would increase the loss of photogenerated electrons before collection. B-rGO in the TiO_2 photoanode is depicted in the energy band and schematic diagrams (**Figure 3**). The element boron is extremely brittle and hard. It is difficult to evenly and precisely deposit it onto the TiO_2 surface using methods like spin-coating, which are frequently employed in

the production of DSSCs. Pure boron is not a good conductor, but boron doping can increase conductivity in reduced graphene oxide (rGO). The conductivity improvement needed for effective charge transport in the DSSC would not be obtained by using pure boron. In addition, depending on the dopant, doping rGO with elements other than boron can introduce distinct functionalities. One popular method that may improve electron injection is nitrogen doping, which adds electron donor sites [Niu, M., Cui, R., Wu, H., Cheng, D., & Cao, D. (2015)]. Multiple oxidation states are introduced by metal doping (transition metals), which may result in multi-step electron transfer pathways [Sufyan et al., 2022]. Improved conductivity and electron transfer may be two benefits of co-doping, which involves mixing boron with other elements (such as nitrogen) [Ngidi, N. P. D., Ollengo, M. A., & Nyamori, V. O. (2019)].

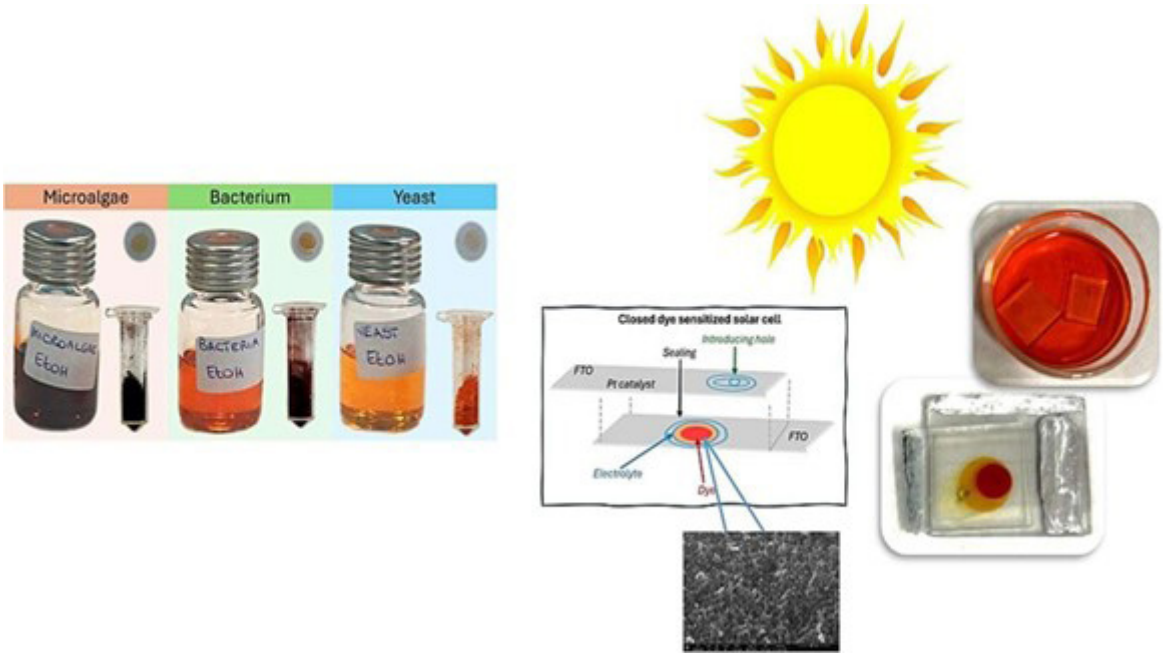
Figure 3. Recombination suppression in dye-sensitised solar cells based on reduced graphene oxide doped with boron and TiO_2 [Mahalingam et al., 2025].



Using a wet chemical method, [Kalaivani et al. 2025] combined graphene and TiO_2 to create a heterojunction as a photoanode for DSSCs. The XRD and TEM results show that the TiO_2 has a tetragonal (anatase) phase and that the graphene sheets are made up of uniformly wrapped spherical nanoparticles with diameters between 30 and 40 nm. In contrast to graphene/TiO_2, which has a bandgap energy of 2.77 eV, anatase typically has a bandgap energy of 3.15 eV for TiO_2. Graphene/TiO_2 DSSCs work 2.22% better than cells based on pure TiO_2 electrodes, with a power conversion efficiency (PCE) of 7.2%. Specifically, by increasing the light harvest of dye molecules, graphene's capacity to absorb solar light may enhance the power conversion efficiency of DSSCs. Furthermore, the average electron transit time for graphene/TiO_2 was 1.765 ms, whereas the average for TiO_2 was 2.981 ms. To the best of our knowledge, no prior research has been conducted on the development of DSSCs using extracts derived from other astaxanthinproducing microorganisms. However, prior studies have been conducted on the development of DSSCs using Haematococcus pluvialis astaxanthin-rich extract as photosensitizer [Orona et al, 2017], [Khan et al, 2023].

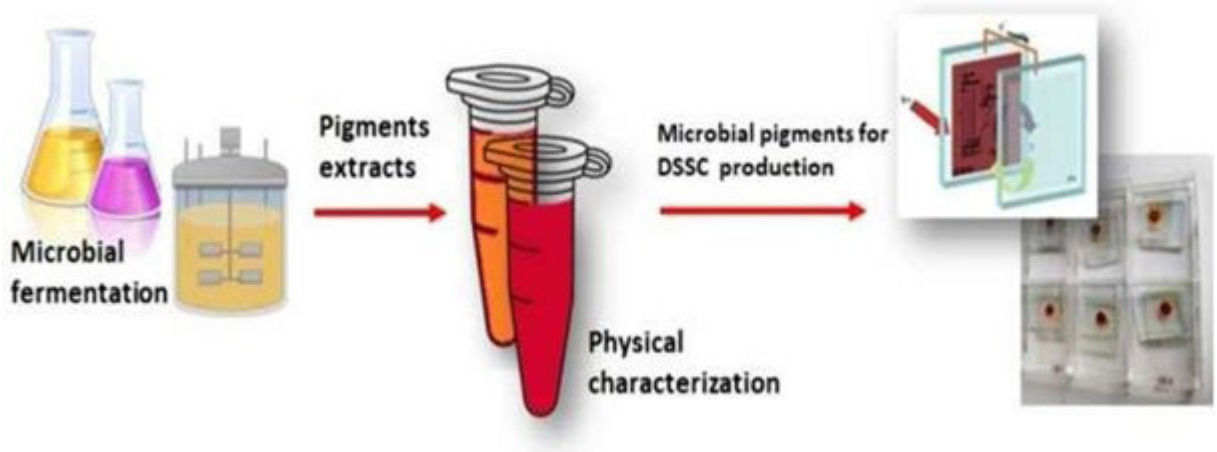
To assess dye-sensitised solar cells' (DSSCs) photovoltaic performance, Tropea et al. (2025) present a novel comparison of astaxanthin derived from three distinct microbial sources. Pigments extracted from the microalga Haematococcus pluvialis, the yeast Phaffia rhodozyma, and the bacterium Paracoccus carotinifaciens were thoroughly characterised using a variety of analytical techniques (HPLC-DAD-APCI-MS, UV–vis spectroscopy, scanning electron microscopy (SEM), IV measurements, and electrochemical impedance spectroscopy (EIS) to highlight the structural variations that affect the dyes' photoelectrochemical behaviour. Based on the extract from Paracoccus carotinifaciens, the DSSC showed the highest efficiency, with a power conversion efficiency (PCE) of 0.36%, an open-circuit voltage (Voc) of 0.419 V, a fill factor (FF) of 0.3, and a short-circuit current density (Jsc) of 2.86 mA/cm2. As seen in **Figure 4**, the devices were put together and the photoanodes were sealed with the CE using a thermopress and a Surlyn gasket (Meltonix 1170–25, Solaronix SA).

Figure 4. The impact of microbiological origins on the use of astaxanthin as a sensitizer in dyesensitized solar cells (DSSCs) [Tropea et al 2025].



The possibility of using extracellular microbial pigment extracts produced by T. atroroseus GH_2 cultivation as appropriate dyes for the application of DSSCs was investigated by Tropea et al. in 2024. In addition to the industrial use of these pigments that has already been studied, the current study enables us to expand their use in the energy sector by using them in solar cell applications. Fermentation was used to grow the fungus, and HPLC-DAD-ESI-MS analyses were used to characterise the extracellular pigment extract. Out of the 22 azaphilone-type pigments that were found, PP-O was the most prevalent compound. To confirm the stability of the schedule and the photovoltaic performance, the behaviour of the device was examined about pH and electrolyte. UV-vis measurements were used to characterise the devices and confirm the transmittance percentage and absorbance intensity. Additionally, impedance characteristics were ascertained by Electrochemical Impedance Spectroscopy (EIS), and photovoltaic parameters were ascertained by photo-electrochemical measurements (I–V curves). The optimal microbial device had an opencircuit photovoltaic (Voc) of 0.27 V, a fill factor (FF) of 0.60, and a short-circuit current density (Jsc) of 0.69 mA/cm^2. Additionally, the device's power conversion efficiency (PCE) was 0.11%. Therefore, the current study showed that microbial origin pigments have the potential to be used in the development of DSSCs **Figure 5**.

Figure 5. creation of dye-sensitised solar cells with Talaromyces atroroseus GH2 pigment extracts [Tropea et al, 2024].

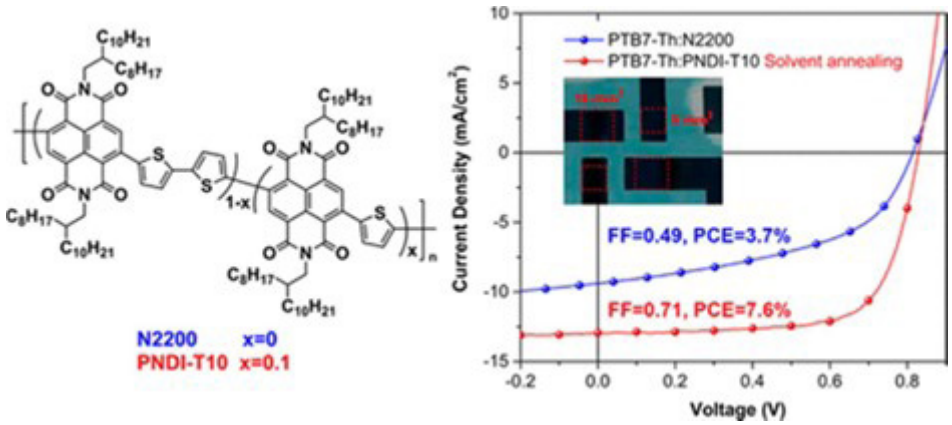


POLYMER SOLAR CELLS (PSCS)

Using conjugated polymers for both polymer donors and acceptors in the active layer, all-polymer solar cells (all-PSCs) have many advantages, including exceptional mechanical flexibility, long device life, and compatibility with roll-to-roll manufacturing. Polymerised small-molecule acceptors have recently become important players in the development of all-PSCS, especially in terms of improving power conversion efficiency. However, the search for high-performing and reasonably priced polymer donors for all-PSCSs continues, creating a production bottleneck on a larger scale. Polythiophene and its derivatives (PTs) have attracted renewed interest because of their affordability, scalability, and ease of use. One promising path toward obtaining high efficiency, low cost, and improved stability in organic solar cells is the development of PT-based all-PSCs [Sun, H., Wang, W., Chen, J., Bai, Q., and Cheng, Y. (2024)]. The flexible, affordable, and lightweight nature of polymer solar cells (PSCs) has drawn a lot of attention. As a result, numerous studies have concentrated on the bulk heterojunction (BHJ) structure of polymerfullerene or fullerene-free PSCs [Fonteyn et al., 2020]. [Samajdar, D. P., & Arefinia, Z. (2021)].The design of polymer acceptors as a possible substitute for fullerene derivatives in highperformance all-polymer solar cells (all-PSCs) has drawn increasing attention. The low fill factor (FF) (typically <0.65), which is closely linked to the mobility and film morphology of polymer: polymer blends, is a major factor limiting the efficiency of all-PSCs.

[Li and others, 2016] By substituting a specific number of bithiophene (2T) units in the N2200 backbone with single thiophene (T) units and creating a sequence of random polymers PNDI-Tx, where x is the percentage of the single T, one can easily alter the crystallinity of the well-known naphthalene diimide (NDI) based polymer N2200. The low band gap donor polymer PTB7-Th and the acceptor PNDI-T10 are suitably miscible, and the nanostructured blend facilitates effective charge transport and exciton dissociation. Higher hole and electron mobilities are made possible by solvent annealing (SA), which also further inhibits bimolecular recombination. The PTB7-Th: PNDI-T10 solar cells achieve a high PCE of 7.6%, which is a twofold increase over the PTB7-Th: N2200 solar cells, as anticipated. The highest value among all-PSCs to date is reached by the FF of 0.71, see **Figure 6**. A novel method employing an alternative polymerisation technique is presented by [Yu et al., 2024]. It is discovered that the unique “double-decker” molecular conformation of the resulting electron acceptor, PffBQx-T, improves device performance. Consequently, ternary all-PSCs with PffBQx-T as a guest achieved an exceptional 18.7% efficiency. This study shows how this novel polymerisation technique can be used to create allPSCSs that are stable and incredibly effective.

Figure 6. Optimized Crystallinity and Solvent Annealing Work Together to Create High-Performance All-Polymer Solar Cells [Li, Z., Xu, X., Zhang, W., Meng, X., Ma, W., Yartsev, A., Inganäs, O., Andersson, M. R., Janssen, R. A. J., & Wang, E. (2016)].



ORGANIC SOLAR CELLS (OSCS)

Organic solar cells (OSCs) have garnered a lot of interest recently due to their many benefits, which include easy preparation, low cost, light weight, and large-area flexible fabrication. Inadequate device stability is still a major problem, even though power conversion efficiencies have surpassed 10%. the elements that restrict OSC stability, including metastable morphology, diffusion of electrodes and buffer layers, oxygen and water, irradiation, heating, and mechanical stress, and examine recent developments in methods to improve OSC stability, including material design, active layer device engineering, using inverted geometry, optimizing buffer layers, employing stable electrodes, and encapsulation. To help readers grasp the difficulties and possibilities in attaining high efficiency and high stability of OSCs towards future industrial manufacture, some device stability research areas that might merit more attention are also covered [Cheng, P., & Zhan, X. (2016)].

The advantages of organic solar cells (OSCs) include their semitransparent nature, flexibility, low cost of fabrication, and low weight [Guo, W., Xu, Z., Zhang, F., Xie, S., Xu, H., & Liu, X. Y. (2016)]. OSCs have garnered a lot of research interest lately, and many researchers are focused on enhancing the device's stability and power conversion efficiency (PCE) [Duan, L., Science, A. U.A., & 2020]. The single-junction and tandem OSCs' PCEs were 18.22% and 17.36%, respectively, a short while ago [Liu et al, 2020]. OSCs have the potential to be used in buildings or cars to generate electricity as windows or curtains because of their semi-transparent (ST) property [Tian et al. 2015]. Building-integrated photovoltaic (BIPV) technology is increasingly emerging as one of the most effective methods for supplying buildings with renewable energy, particularly in the building sector. There is potential for the extensive integration of ST-OSCs into greenhouses, windows, and building facades. The semi-transparent property of ST-OSCs enables them to function as a generator while simultaneously lowering electricity consumption by allowing natural light to flow through [Joseph, B., ... T. P.-I. J. of, & 2019]. OSCs have the potential to be used in buildings or cars to generate electricity as windows or curtains because of their semi-transparent (ST) property [Tian et al. 2015]. Building-integrated photovoltaic (BIPV) technology is increasingly emerging as one of the most effective methods for supplying buildings with renewable energy, particularly in the building sector. There is potential for the extensive integration of ST-OSCs into greenhouses, windows, and building facades. The semi-transparent property of ST-OSCs enables them to function as a generator while simultaneously lowering electricity consumption by allowing natural light to flow through [Joseph, B., ... T. P.-I. J. of, & 2019]. Nevertheless, they have less contribution to the energy conversion process in However, because most organic materials have a limited absorption spectrum, they contribute less to the energy conversion process in OSCs. The development of new flexible bottom or top transparent electrodes, the design and synthesis of high-performance photoactive layer and low temperature processed electrode buffer layer materials, and device architecture engineering have all contributed to the rapid development of flexible and semitransparent OSCs in recent years. The highest power conversion efficiencies to date have been over 10% for flexible OSCs and 7.7% for semitransparent OSCs, with an average visible transmittance of 37%. A thorough review of current research developments and viewpoints on the associated materials and devices of the flexible and semitransparent OSCs is given in [Li, Y., Xu, G., Cui, C., & Li, Y. (2018)].

Because they are inexpensive to produce, polythiophenes (PTs) hold great promise as electron donors for organic solar cells (OSCs). However, because of their unmatched energy levels and unfavorable active layer morphology, PTs perform poorly as devices in OSCs. To achieve highefficiency OSCs, [Yuan et al. (2022)] report a set of new PTs (P5TCN-Fx) with varying fluorination degrees and cyano-group substitutions. The new PTs are endowed with deep-lying energy levels by the cyano-group's incorporation, and their backbone fluorination results in enhanced polymer crystallinity, strong interchain interaction, and suitable thermodynamic miscibility with the dominant acceptor Y6. Wang and colleagues (2019). Consequently, more than sixteen percent efficiency in binary OSCs has been provided by several PTs. Furthermore, P5TCNF25 achieved a notable PCE of 17.2% through ternary blend design, setting a new efficiency record and marking a significant advancement for PT-based OSCs. A promising path toward producing high-performance OSCs from inexpensive materials is made possible by this work. In order to achieve high-performance NFA-based OSCs with PTs as electron donors, a number of crucial factors must be addressed. Because the thiophene ring is electron-rich, PTs typically have high-lying highest occupied molecular orbital (HOMO) levels (about −5.0 eV). This makes it challenging to match the deep-lying lowest unoccupied molecular orbital (LUMO) levels (about −4.1 eV) of the dominant NFAs. Thus, a low open-circuit voltage (V_{OC}) in OSCs was caused by the mismatch in energy levels between PT and NFA. According to Yang et al. (2020), the most advanced NFAs typically have absorption spectra that reach the near-infrared region and narrow optical band gaps. Consequently, to achieve a high short-circuit current density (J_{sc}), the light absorption of PTs and NFAs should be complementary. Because PT and NFA are hyper-miscible, PT-based OSCs had intimately mixed active layer morphology without phase separation, which limited the Jsc and fill factor (FF). There had been some attempts to resolve these problems. Hou et al., for instance, reported a new NFA by altering the end group to adjust the miscibility between poly (3-hexylthiophene) and NFA. The resulting OSCs had a PCE of 9.46%, but the possibility of achieving higher PCEs was constrained by the NFA's primarily blue-shifted absorption spectrum. [Yang and others, 2020]. Creating new PTs that correspond with the current NFAs is an additional tactic. However, when combined with the existing NFAs, the PTs that match fullerene acceptors and A-D-A type NFAs showed extremely poor device performance [Liang and others, 2020]. In stark contrast to the respectable PCE of 12.1% provided by the PDCBT-Cl:ITIC-Th1 blend, a PT derivative, PDCBT-Cl, yielded an incredibly poor PCE of 0.5% when blended with Y6. [Su et al 2024]The highly mixed active layer morphology is the main cause of the PDCBT-Cl: Y6 device's subpar performance. To achieve high-efficiency OSCs, new PTs with complementary light absorption, matched energy levels, and suitable thermodynamic miscibility with the most advanced NFAs must be designed [Jia et al 2019]. report the synthesis of three new polythiophene derivatives (P4T2F-HD, P4T2F-HD/BO, and P4T2F-BO) using a three-step reaction.

In solution, the polymers exhibit the desired aggregation properties and outstanding coplanarity. In comparison to the commercial polymer poly (3-hexylthiophene) (P3HT), the new polymers' HOMO energy levels were down-shifted by 0.4 eV. Both fullerene and non-fullerene acceptors can be used with the polymers to provide high device performance. A non-fullerene acceptor (5Z,5'Z)-5,5'-((4,4,9,9tetraoctyl-4,9-dihydro-s-indaceno[1,2-b:5,6-b']dithiophene-2,7-diyl) when combined with itP4T2F-HD provides the highest PCE of 7.0% with a high V_{OC} of 1.04 V for bis(benzo[c][1,2,5]thiadiazole-7,4-diyl)) bis-(methanylylidene))bis(3-ethyl-2-thioxothiazolidin-4one) (O-IDTBR). Furthermore, when combined with a fullerene acceptor, P4T2F-HD can withstand a wide range of active layer thickness variations [Cai and others, 2025].

Since single-junction OSC efficiencies have surpassed 19%, OSC commercialisation is becoming more promising. A crucial step towards the commercialisation of OSCs is the fabrication of largearea printing, and solution-processed, thickness-insensitive cathode interlayers (CILs) are desperately needed for this purpose. For thickness-insensitive CILs to be possible, cathode interfacial materials (CIMs) must have high electron mobility. High electron mobility can be conferred on organic CIMs by N-type self-doped properties. The applicability of various n-type self-doped CIM types in conventional and inverted OSCs varies. The electron mobility of hybrid blends can be further enhanced by external n-type dopants. Inverted OSCs can achieve superior photoconductivity, especially when ZnO is doped with organic dyes.

PEDOT FOR ORGANIC SOLAR CELLS

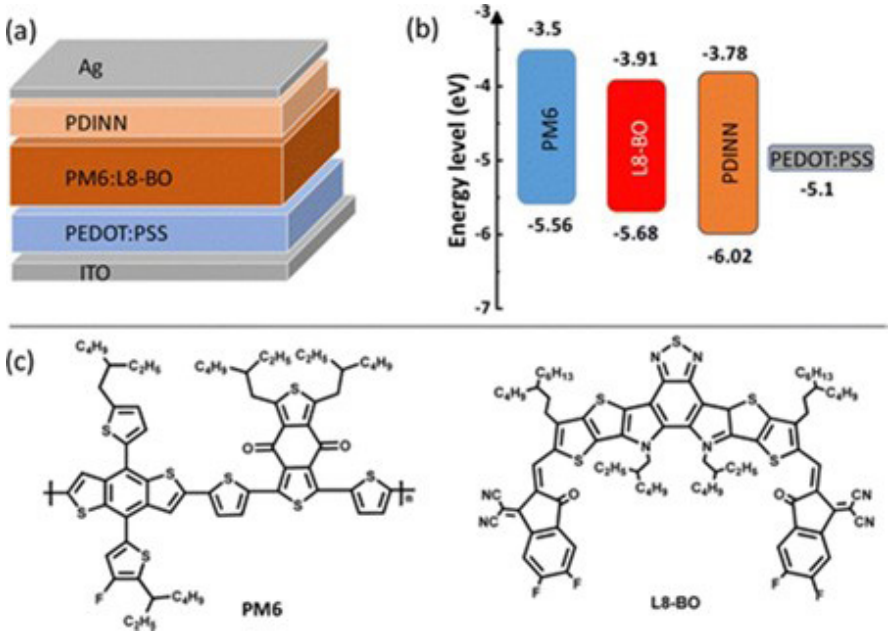
The development of organic electronics depends on an understanding of the critical elements affecting the stability of organic solar cells (OSCs) [Yao et al. 2024] To reveal for the first time how the quality of PEDOT hole transporting materials (HTMs) affects the thermal stability of OSCs, a variety of poly (3,4-ethylenedioxythiophenes) (PEDOTs) with different molecular weights (Mw) and doping levels (DL) were synthesized. Higher Mw and DL values are demonstrated to be more effective in maintaining the p-doping properties of PEDOTs throughout thermal ageing, allowing the HTM to exhibit more stable electrical properties (i.e., work function and conductivity). Conversely, poor-quality PEDOTs encourage the development of bigger crystalline structures in the active layer, which makes them more prone to breaking down as a result of thermal ageing. As evidenced by a low efficiency decay rate of about 28%, both effects help to achieve exceptional device stability [Liu, et al 2024] rationally designed an unsymmetrical interfacial phosphonic acid, BrDECz, by introducing an electron-donating and an electronwithdrawing group through straightforward coupling reactions for a push–pull self-assembled monolayer/multilayer (SAM). We systematically show that the unsymmetrical structures induce a larger dipole moment, optimised energy levels, higher adsorption energy, and enhanced conductivity, as confirmed by KPFM and C-AFM measurements. These factors collectively contribute to enhanced charge extraction and collection as demonstrated by transient technologies. Consequently, we achieved a 19.67% PCE in binary single junction OSCs, one of the highest reported efficiencies for this type of device. Importantly, the designed unsymmetrical BrDECz interfacial layer is universally applicable to other systems and offers improved thermal stability compared to PEDOT: PSS. The unsymmetrical interfacial molecule strategy offers valuable insights into the design and application of interfacial materials, presenting a promising approach for further enhancing the photovoltaic performance of OSCs.

Here, we aim to investigate the effects of temperature changes on the efficiency of inverted bulk heterojunction (BHJ) OSCs [Chen, Z., El, M., Boudia, A., & Zhao, C. (2025)]. Through some mechanisms, temperature variation has a significant impact on the efficiency of inverted bulk heterojunction OSCs. While higher temperatures can improve charge carrier mobility in inverted BHJ OSCs, they can also result in higher recombination rates, lower Voc, and possible material degradation. Improving OSCs' thermal stability and efficiency, particularly for applications in a variety of environmental conditions, requires an understanding of and commitment to optimising these factors. The performance and thermal stability of these OSCs are examined through simulations employing three distinct electron transport layers: SnO_2, C60, and PC60BM. Particular attention is paid to analyses of their high thermal stability (measured by the PCE loss ratio) at 350 K under a high PCE of about 20%. In lab settings, this might result in the creation of OSCs that are more stable and effective. As far as the reader is aware, these are unique structure models with a 4.84 mm^2 device area that were created and executed in response to an earlier study by [Zhu et al. 2022].

Using an active layer system of PM6: L8-BO, [Li et al. 2024] created organic solar cells and carried out a thorough investigation into the performance impacts of thermal annealing, additive treatment, and active layer thickness. Simple procedures and inexpensive interfacial materials produced optimal binary OSCs with a PCE of 18.33%, a Voc of 0.881 V, a Jsc of 26.56 mA cm^{-2}, and an FF of 78.33%. According to AFM, GIWAXS, and other characterization results, the photovoltaic performance of PM6:L8-BO solar cells can be improved by optimizing the active layer morphology, improving charge transport and extraction, balancing light absorption, and improving the interface contact between the active layer and the electrode by adding additives to the active layer, applying thermal annealing at the right temperature, and controlling the thickness. The schematic diagram of the

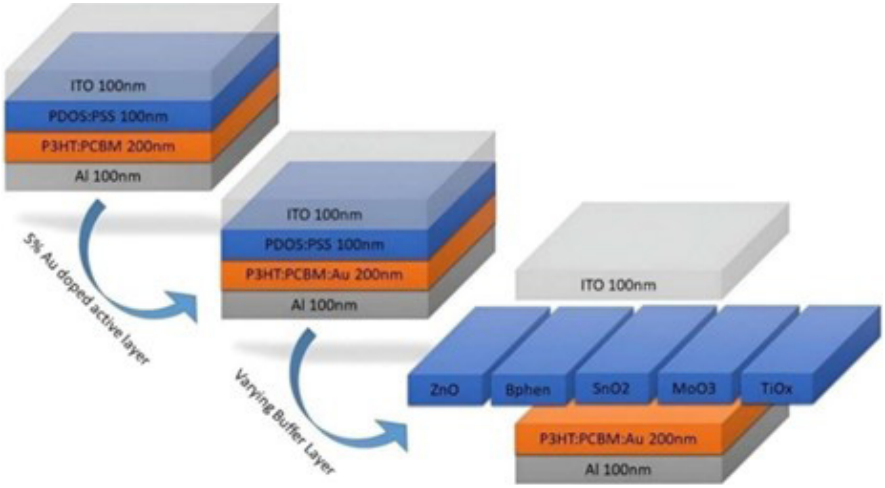
device structure ITO/PEDOT/PM6:L8-BO/PDINN/Ag is displayed in **Figure 7(a)**. The chemical structures of the polymers PM6 and L8-BO are displayed in **Figure 7(c)**. In this work, a donor (PM6) and an acceptor (L8-BO) were chosen and utilised. The energy level diagram in **Figure. 7b** shows how a distinct energy arrangement forms between the various layers, facilitating efficient charge transfer [Benaya, et al (2025)].

Figure 7. (a) The BHJ OSC's schematic device structure. (b) Alignment of the device's materials at the energy level. (c) The chemical makeup of the non-fullerene acceptor L8-BO and polymer donor PM6 [Li, et al 2024].



It has been shown that adding 5% gold nanoparticles (Au NPs) to the P3HT active layer greatly improves the efficiency of organic solar cells (OSCs). According to simulation results, devices with Au NPs had a significantly higher power conversion efficiency (PCE) than devices without Au NPs, with PCEs up to 6.46 percent when BPhen was used as the hole blocking layer (HBL). Additionally, while maintaining a high fill factor (FF) of 68 percent, the addition of Au NPs improved other important photovoltaic parameters, such as the short-circuit current density (Jsc), which increased from -12.01 mA/cm^2 to -15.55 mA/cm^2. The impact of various HBL materials on device efficiency was also highlighted by the study; BPhen was found to be the most effective HBL, outperforming ZnO and TiOx, which had somewhat lower PCE values of 6.38 and 6.40 percent, respectively. These results show that the performance of the device is significantly improved when Au NPs and optimised HBLs, especially BPhen, are combined. At 300 K, the OSC configuration was investigated in the AM1.5 spectrum. Important electrical parameters of the solar cell are then extracted from the obtained current density–voltage (J-V) curves. These parameters consist of FF, η, Voc, and Jsc. As illustrated in **Figure. 8**, where panels (a) and (b) show the materials used for various active layers with the same layer thickness, OSCs were the subject of this investigation. Figure 8 contains: PSS (HBL)/P3HT: PCBM (Hybrid p-n layer)/Al and PSS (HBL)/P3HT: PCBM:Au 5% (mixture of p-n layer with additional nanoparticles) are the substrates/ITO/PEDOT.

Figure 8. The proposed structural model of the OSCs under study, along with every layer included in the simulation. [Benaya, et al (2025)].



GEL POLYMER ELECTROLYTE

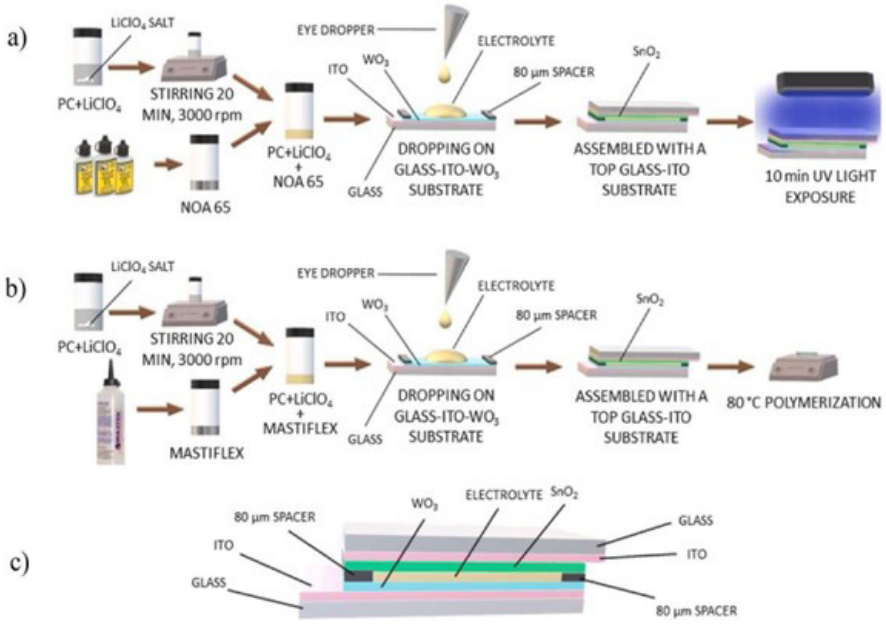
In a GPE, the polymer chains form a network with interconnected pores that facilitate the absorption of the liquid electrolyte and enable charge transfer. GPEs can be prepared using two different methods, depending on the nature of the preparation process. One method involves using a porous polymer matrix that allows the liquid electrolyte to be absorbed through swelling. Porous structures in the polymer matrix can be achieved through the controlled removal of a solvent from a polymer solution or by directly forming fibrous structures with inherent porosity. The other method involves storing the liquid electrolyte between polymer chains generated via in situ polymerisation. The common methods used for preparing GPEs include solution casting, phase inversion, and in situ polymerisation. These methods are considered energy-efficient, costeffective, and environmentally friendly compared to other available methods for GPE preparation.

Gel Electrolyte for Solid-State Cell

One essential part of a dye-sensitised solar cell (DSSC) is the electrolyte system [M. O. S. Lobregas and D. H. Camacho (2019)]. Here, a possible quasi-solid-state electrolyte system for DSSC is described: a gel polymer electrolyte (GPE) based on starch. To create the cationic starch (CS), which has a nitrogen content of 1.33% (degree of substitution = 0.084), 1-glycidyl-3methylimidazolium chloride (GMIC) ionic liquid was grafted onto the potato starch backbone. Changes in the molecular structure, morphology, and thermal behaviour were used to identify the successful modification. The flaky morphology and high water solubility of CS set it apart from the raw starch's granular morphology and water insolubility. A gel with the highest conductivity and the most effective ion migration was achieved by optimising the gel polymer electrolyte (GPE) system concerning the CS:GMIC ratio (1:3) and the weight percentage of KI/I2 (70%) redox couple. A dye-sensitised solar cell (DSSC) with an efficiency of 0.514% was created using the optimised CS-GPE as the quasi-solid-state electrolyte system. Because of its good filling contact between the electrodes, it demonstrated relative stability despite performing poorly when compared to the liquid electrolyte control [Primiceri et al., 2022].

Two less expensive and non-toxic commercial resins are used to prepare a gel polymer electrolyte (GPE): a vinyl acetate-based resin (MASTIFLEX) and a prepolymer based on urethane (NOA65). They are used as host matrices, composed of lithium perchlorate-propylene carbonate (LiClO4PC), to trap the liquid constituents. Both resins exhibit outstanding thermal performance, according to thermogravimetric analyses. Several GPE formulations with different $LiClO_4$ concentrations and polymer-to-liquid ratios are examined in terms of their electrical and optical characteristics. The optical contrast, switching kinetics, and repetitive switching cycles of the EC devices constructed using the two GPEs are also described. The best formulations were ultimately used to fabricate 100 cm^2 large area EC devices thanks to these efforts. As ion-conducting media for EC devices, the obtained results show that inexpensive GPEs based on commercial polymers are electrochemically stable. To test the developed GPEs in an EC system, solid state devices were constructed following the schemes depicted in Figure. 9 following the initial characterisation activities. An ITO/WO_3 working electrode and an ITO/SnO_2 counter electrode were then positioned between each GPE (from "a" to "l" for NOA65 and from "A" to "L" for MASTIFLEX). This outcome is consistent with the increased ion conductivity values shown in **Figure 9**.

Figure 9. Manufacturing procedures for EC devices for MASTIFLEX (b) and NOA 65 (a). (c) Diagrammatic representations of the architecture of the EC device [Primiceri, et al 2022].



By including a methodical experimental study of how gel electrolytes affect the characteristics of partially covered photoelectrochromic devices [Theodosiou, Dokouzis, A., Antoniou, I., & Leftheriotis, G. (2019)]. Different concentrations of poly (methyl methacrylate), PMMA (Mw 120.000), ranging from 0% w/w to 45% w/w, dissolved in acetonitrile with 0.5 M lithium iodide, 0.005 M iodine, and 0.5 M 4-tert-butylpyridine, were used to create a series of gel electrolytes. The electrolytes' ionic conductivity decreased as the PMMA concentration increased, and it was on the order of 10^{-5} S/cm. These electrolytes were integrated into photoelectrochromic devices that were partially covered. It was discovered that the power conversion efficiency of the integrated solar cells drops (from 1.7% to 0.5%) as the concentration of PMMA increases. This is primarily because the short-circuit current decreases. Up to 35% w/w PMMA concentration, the devices' colouration kinetics, photocoloration efficiency, and PhCE were almost constant; as the PMMA concentration increased, they became less so. Because it produces devices with acceptable electrical and optical properties, the electrolyte with a 35% w/w concentration of PMMA was preferred among those tested.

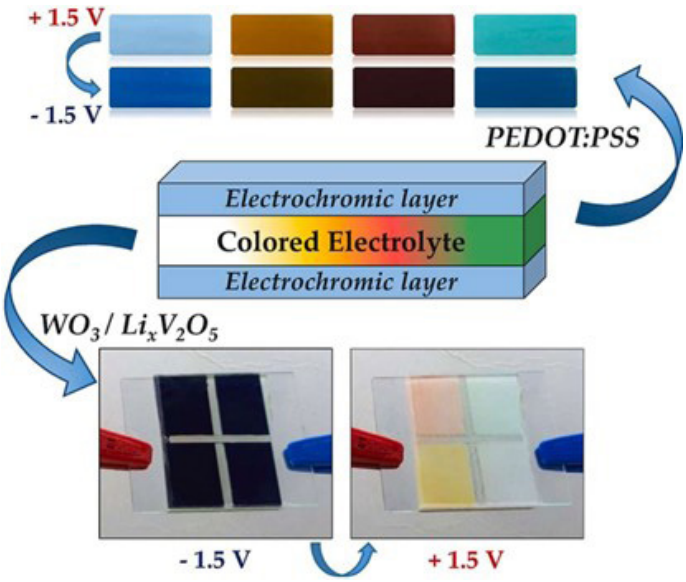
Gel Polymer Electrolyte for Color Cell

In 2012, [Watanabe, Y., Nagashima, T., Nakamura, K., & Kobayashi, N.] synthesized solid-state electrochromic (EC) cells with a gel electrolyte and phthalate derivatives. Via electrochemical reactions, the cells displayed striking color changes, changing from water-transparent to one of the three primary colors (yellow, magenta, or cyan). Furthermore, we used the three primary-color EC cells to produce continuous-tone images. Applying a rectangular-wave voltage with different duty ratios allowed the EC cells to create continuous-tone images.

In [Périé, C., Mary, V., Faceira, B., & Rougier, A. (2022), a novel method of color modulation— the electrolyte coloration is examined. As a result, the color tuning is not solely caused by electrochromic materials; it is also addressed by the addition of pigment to the electrolyte, opening up countless possibilities. To describe this coloration process, a WO_3//V_2O_5 display and a symmetrical PEDOT:PSS based display were developed. Four distinct pigments were used to color the PEGDMA/PEGMA copolymer gel electrolyte after it had been thermally polymerized using AIBN. Comparable capacities and switching times were recorded for each colored electrolyte. This simple setup technique increases the number of colors that can be achieved without compromising the stability of the electrochromic device. **Figure.10**.

In 2018, Zhou, J., Wang, J., Li, H., and Shen, F. A hybrid gel polymer electrolyte (GPE) based on poly (propyleneglycol) bis(2-aminopropyl ether) (2-APPG) and 3-isocyanatepropyltriethoxysilane (ICS) was successfully synthesized by the sol–gel method using propylene carbonate (PC) as the solvent. The hybrid gel polymer electrolyte with a [O]/[Li] ratio of 22 has good thermal stability, good electrochemical stability, and high ionic conductivity, according to the results. At 30 °C, the ionic conductivities can reach 1.43×10^{-3} S cm^{-1}, and at 100 °C, they can reach 3.36×10^{-3} S cm^{-1}. There was almost no weight loss up to 100 °C. The hybrid gel polymer is used as the electrolyte in the fabrication of the electrochromic device. When the applying voltage is increased to as high as 5 V on the electrochromic device, a fast response is obtained (colored/bleached time is 13/19 s), indicating its potential application under high voltage conditions. The results show its high coloration efficiency (267.4 cm^2 C^{-1}) and long cycle life (150 cycles with the linear potential sweep between − 3.5 and + 2.5 V).

Figure 10. Electrolytes with color for electrochromic devices [Périé, C., Mary, V., Faceira, B., & Rougier, A. (2022)].



POLYMER BLENDING STRATEGY

A polymer blend is defined in the literature as a mixture of at least two macromolecular substances, either copolymers or polymers, at a relative concentration greater than 2 weight percent [Utracki, L 2013]. The potential to create new polymers with customized properties that differ from those of the constituents, thereby resolving technical issues brought on by the synthesis of novel matrices, is the reason for the steadily growing interest in polymer alloys [Mantia et al., 2017]. To put it another way, polymer blend technology offers materials with all the desired (or enhanced) qualities at a low cost. It also presents a novel strategy for the effective recycling of plastic waste from businesses and/or municipalities. The potential for increased versatility and processability, along with a decrease in the number of grades that must be produced and stored, is what has plastics manufacturers interested in these

materials. The application of roughly 39% of the polymers in composites and 36% in blends can be explained by these factors. Polymer manufacturers create about 65% of polymer alloys, compounding companies make about 25%, and transformers make the remaining 10% [Utracki, L., & Wilkie, C.2002].

These blends can generally be made using five different manufacturing processes: partial block or graft copolymerization, latex mixing, melt compounding, solution blending, and synthesis of interpenetrating polymer networks. Due to the use of well-defined components and the versatility of the mixing devices, the most widely used transformation technology for polymer alloys is the mixing of the blend components in the molten state using melt compounders like screw extruders. Polymeric materials that are mechanically strong and resilient are highly sought after for a variety of applications, from flexible electronics to aerospace. However, because polymers are inherently contradictory, it is still very difficult to achieve both high toughness and strength.

The performance of CMSMs in gas separation is largely dependent on their precursor. Researchers have identified polymer blending, modification, and doping with inorganic particles as important ways to improve gas separation capabilities in addition to polymer types. The most popular technique for creating hybrid matrix membranes is mixing or physical blending. The continuous phase of these membranes is a polymer matrix, while the dispersed phase is a filler. Fillers generally fall into one of the following categories: inorganic (graphene oxide, carbon nanotubes, MXenes, etc.), ceramic (silica, zeolite, alumina, etc.), organic-inorganic hybrid (metal-organic skeleton, covalent organic skeleton, etc.), or polymer blends (polymers, organic compounds, etc.) [Aframehr, et al 2020].Organic photovoltaic cells (OPVs) that are intrinsically stretchable have attracted a lot of interest as essential components for supplying energy to wearable electronics of the future. Even though champion OPVs have seen quick increases in power conversion efficiency, their brittle stretchability has not kept up with the demands of the Internet of Things era, which has seriously hampered future research and useful applications [Xin, J., Liu, Y., Zhao, B., & Chen, Z. A. (2024)].

A new mixing technique is suggested for precisely segment-level mixing of polyimide-co-siloxane (PSI) blends in order to optimize the structures and gas separation characteristics of carbon molecular sieve membranes (CMSMs). PSI copolymers with varying siloxane contents were created and mixed; they were designated PSI-0, PSI-1, PSI-2, and PSI-3 according to the DABA:siloxane molar ratios of 10:0, 9:1, 8:2, and 7:3, respectively. With a focus on the gas separation capabilities of CMSMs, this study aims to clarify the complex interactions between the distribution of repeating segments and the resulting carbonization structures. Particularly noteworthy is the PSI-0:PSI-3 (1:2) blend, which produces a CMSM with comparable hydrogen permeability and significantly improved selectivity (232 % H2/CH4 and 184% H2/N2 selectivity) even though it contains the same amount of siloxane as neat PSI-2. In [Li et al. 2024], a novel high-molecular-weight conjugated polymer PM6-HD is designed in order to demonstrate a new dual-donor polymer blending strategy for creating intrinsically stretchable OPVs. This PM6 derivative with long alkyl chains has a high fracture strain of over 90%, which is about 12 times greater than the benchmark PM6, because it can reach a high enough molecular weight. In polymer:small molecule and all-polymer systems made from the physical blends of PM6 and PM6-HD, synergistic optimization of mechanical properties and photovoltaic performance is accomplished. Importantly, even after 1000 cycles of cyclic stretching at high strains, the resulting intrinsically stretchable OPV exhibits exceptional stretchability and stability, with a record PCE80% strain of 50.3% and an efficiency retention of above 80% [Ma and others, 2024] It is commonly known that two structurally similar polymer acceptors can be used to create high-efficiency ternary all-polymer solar cells. However, up until now, there hasn't been much attention paid to how the polymer acceptor or acceptors would adjust the aggregation of polymer donors, as well as film morphology and device performance (efficiency and stability). According to this report, matching the donor PBQx-TCl with the celebrity acceptor PY-IT leads to improved H-aggregation in PBQx-TCl. This can be adjusted by varying the quantity of the second acceptor PY-IV. A state-of-the-art power conversion efficiency of 18.81% is thus achieved with the efficiency-optimized PY-IV weight ratio (0.2/1.2), which also improves well-protected thermal stability and light-illuminated operational stability.

The use of ligand-modulated metal–organic framework (MOF) nanoparticles, which are designed to have adjustable hydrophilicity and lipophilicity by varying the types and ratios of ligands, is presented in [Kuang et al. 2024]. These nanoparticles can efficiently control the interfaces between chemically different polymers according to their amphiphilicity, as shown by molecular dynamics (MD) simulations. Interestingly, a 0.1 weight percent addition of MOF nanoparticles with optimized amphiphilicity (ML-MOF(5:5)) increased the strength and toughness of the poly (lactic acid) (PLA)/poly (butylene succinate) (PBS) blend by approximately 1.1 and 34.1 times, respectively. Furthermore, the mechanical properties of a variety of polymer blends, including PLA/poly (butylene adipate-co-terephthalate) (PBAT), PLA/polypropylene (PP)/polyethylene (PE), PP/polystyrene (PS), and PLA/polycaprolactone (PCL)/PBS, are universally improved by these amphiphilicity-tailorable MOF nanoparticles. This simple universal method offers significant potential for strengthening and toughening various polymer blends.

Figure 11. A novel segment-level mixing technique to enhance the carbon molecular sieve membrane's gas separation capabilities made from polymer blends [Chen, Z. A., Zhao, B., Xin, J., & Liu, Y. (2024)].



PHOTOVOLTAIC (PV) AND ORGANIC PHOTOVOLTAIC (OPV)

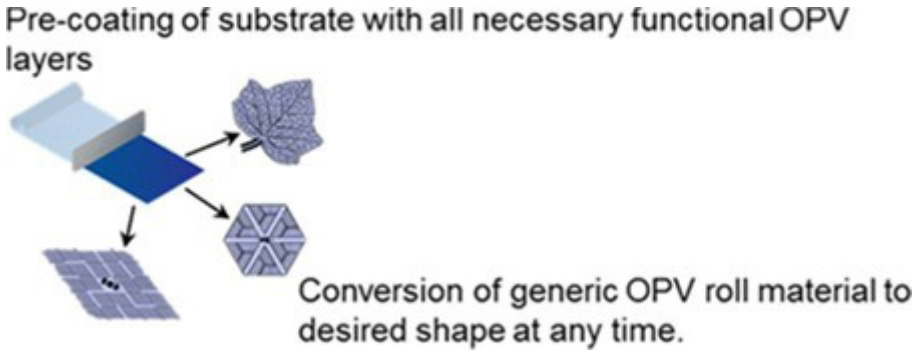
Among solar energy conversion technologies, photovoltaics (PV) is the most mature and rapidly expanding worldwide [Gorjian, S., Calise, F., Kant, K., ... M. A.-J. of C., & 2021]. With a production capacity of almost 107 GW in 2020, PV technology has seized a huge market in the contemporary electricity sector, and solar energy use has seen groundbreaking advancements in recent years across all countries [E. Bellini 2020]. To boost profitability, improve yields, speed up production, and aid in better resource management, photovoltaic technology uses semiconductors to directly convert sunlight into electricity. While the traditional ground-mounted arrangement of PV modules accounts for a large portion of the world's installation capacity, newer installation types such as floating [Gorjian, S., Sharon, H., Ebadi, H., Kant, K., ... F. S.-J. of C., & 2021], building-integrated [Dai, Y., Energies, Y. B.-, & 2020] rooftop [Duman, A., Energy, Ö. G.-R., 2020] also make a substantial contribution. Low carbon emissions, long-term energy sources, high reliability, low maintenance, and a shorter payback period are some advantages of using solar energy technology in crop cultivation settings. The use of PV technology in agriculture is expanding globally, offering environmental sustainability and energy self-sufficiency in growing environments. Farms' energy needs and their potential as energy producers should be taken into account when planning the installation of PV systems. With the highest operational viability in rural regions and remotely accessible agricultural settings such as ranches, orchards, and greenhouses, photovoltaic systems are more cost-effective in distributed electricity generation settings. While central PV power plants are better suited to meet the power demand in larger farms, decentralised PV systems can supply electricity in small-to medium-sized cultivation environments.

One of the most promising solutions to today's energy problems is to use solar energy. Even though inorganic materials are the foundation of the current dominant photovoltaic (PV) technology, their widespread adoption is constrained by high material and manufacturing costs1. Organic photovoltaic (OPV) devices are one of the promising low-cost PV technologies that have been the subject of extensive research. One notable technology is Organic Photovoltaics (OPV), which uses organic photovoltaic film. According to [Kuang et al. (2016)], these cells are made up of organic semiconductor photovoltaic films that are arranged in parallel or series, offering properties that permit a range of sizes and shapes. OPV cells are more efficient than silicon cells, possibly up to 20% more efficient, despite having a shorter lifespan. The partial shading effect is a major problem for OPV cells because it can produce low-resistance paths that harm and eventually render the cell useless. Maximum Power Point Tracking (MPPT) is one technique to anticipate or lessen this effect. I-V curves, which offer comprehensive details about a photovoltaic array's electrical parameters and facilitate performance assessment and monitoring, must be traced to spot possible problems in these components [Barbosa, M. dos S. (2022)].

Organic semiconductors, which are carbon-based materials with backbones primarily made up of alternating C–C and C=C bonds, are the foundation of OPV devices. The semiconducting characteristics of OPV devices are caused by electron delocalisation along the conjugated backbone2. Because of their low dielectric constant ($\hat{G}r \approx 2–4$), organic semiconductors have tightly bonded excitons (electron–hole pairs), which is one of their main differences from inorganic semiconductors. The Frenkel exciton's binding energy falls between 0.3 and 1 eV (Nature, S. F.-, & 2004). In organic light-emitting devices, such a high binding energy can achieve a

high electroluminescent efficiency by preventing exciton dissociation by an electrical field (a non-radiative decay channel). Roll-to-roll printing and other low-cost, large-area deposition technologies are made possible by the weak intermolecular van de Waals interaction. Because of their potential low cost and high performance characteristics, organic electronic devices—such as organic light-emitting diodes (OLEDs), organic thin film transistors, organic photovoltaics (OPVs), and organic memory devices—have garnered a lot of attention in recent years. OLED screens, which are used in gadgets like smartphones, have significantly increased their market share in the portable electronics industry [González, M. O. A., & Sampaio, P. G. V. (2022)]. Furthermore, OPV modules can be shaped into any shape or form thanks to the late-stage customization process [Vishnu et al., 2020]. Free-form organic photovoltaics (OPVs) have emerged as a distinctive feature in contrast to other thin-film OPV technologies. A paradigm shift in traditional energy businesses is brought about by the ability to conform coated layers to any shape or structure, which is revolutionary for OPVs. Modern methods must be used to offset the energy demand as urbanization increases, and OPVs offer special qualities that allow for complete
customization of their form or shape. Because they can be readily incorporated onto structures or even products, this produces a synergy. By doing this, the amount of space needed is reduced, and instead of being transported from central harvesting, the energy is delivered straight to the point of use. The advancements in achieving such free-from patterns through late-stage customization—the process of shaping the functional layers after they have been deposited—are covered in this communication **Figure12**.

Figure 12. Late-Stage Customization in Organic Photovoltaics Volume Production[Vishnu et al 2020].



Moreover, molecular engineering allows for the tuning of OPV absorption wavelengths. Because of these unique characteristics, organic photovoltaics can be used in a variety of applications without having to compete with conventional PV technologies. One of the most promising application areas is building integration, including solar-powered urban furniture or facades and semi-transparent balustrades [Meng et al., 2018]. In these situations, the success of any PV technology depends on the product's customisation and the structures' harmonic integration. Based on whether the molecules that make up OPVs are small or large (polymers), they are separated into two groups. The synthesis, purification, and device fabrication processes of these two material classes differ somewhat. While small-molecule solar cells are primarily processed by thermal evaporation deposition in a high-vacuum environment, polymer solar cells (PSCs) are processed from solution in organic solvents. Although film quality and crystallisation are anticipated to be problems, the solution process has recently gained popularity for creating small-molecule solar cells. Several favourable characteristics7 make PSCs appealing, such as their thin-film architecture, low material consumption due to a high absorption coefficient, use of plentiful organic materials, effective solution processes, and low manufacturing energy requirements. Their high transparency, mechanical flexibility, tunable material properties, and low specific weight are additional benefits [Li, G., Zhu, R., & Yang, Y. (2012)].

Life Cycle Analyses of Organic Photovoltaic

A method for examining a product's environmental effects throughout its life cycle, including the procurement, manufacturing, transportation, and disposal of raw materials, is called life cycle assessment (LCA) [Tsang et al., 2016]. Because the process measures all direct and indirect energy consumed, this approach is beneficial for assessing energy production systems. The goal and scope definition, life-cycle inventory analysis, life-cycle impact assessment, and interpretation steps are the four primary stages of the life cycle assessment (LCA) method.Organic photovoltaic (OPV) technologies are quickly becoming a competitive substitute for conventional thin-film and silicon technologies. According to projections, OPVs will be relatively cheap, have a low energy payback time (EPBT), and produce fewer anthropogenic emissions over the course of their lifetime. [D. Yue, P. Khatav, F. You, & S. B. Darling, 2012].Crystalline silicon solar cells, thin-film solar cells, and new PV technology—a less well-defined group of cutting-edge technologies that surpass the Shockley–Queisser limit—are the first, second, and third generations of photovoltaic cells.The second group includes molecular organic photovoltaic (OPV) cells and polymer cells.

The main reasons for the worldwide interest in creating these OPV cell types are their potential for flexibility, solution coatability, affordability, light weight, semi-transparency, and ease of integration into various applications. The literature outlines potential commercialization paths for devices that use these cells. [Lizin and others, 2013]These paths are mostly predicated on assessments of how performance has changed along with the advancement of technology along the efficiency, lifetime, and cost triangle. If these predictions come to pass, the widespread use of OPV devices could have unanticipated detrimental effects on the environment if it is not adequately evaluated ex ante.Informed choices should ideally be made during the product design phase, indicating that evaluations of the product's components' ecotoxicity, health risks, and life cycle should have been finished before each stage of the life cycle [Agger, A. (2016)].

The efficiency of OPVs is known to be lower [Tsang, M., Sonnemann, G., and, D. B.-S. E. M., & 2016]. And, in contrast to traditional silicon PVs, have shorter lifespans [Lizin et al., 2019]. As a result, the cumulative use and replacement of depleted OPV panels over the course of their service life may outweigh any environmental benefits observed during OPV manufacturing. Furthermore, there are still significant questions about how PV panels will and can be disposed of when their useful lives are coming to an end [Espinosa et al., 2015]. Conventional PVs lack this infrastructure, so landfilling is the go-to remedy. Since OPV panels are not yet commercially available, it is also unclear how they might be disposed of; therefore, it is crucial to predict how disposal methods will affect the technologies' life-cycle effects. Such analyses are expanded beyond the manufacturing stage by [Tsang et al. (2016)], which assesses the potential cradle-to-grave life-cycle impacts of organic photovoltaics in comparison to conventional ones. Two systems (a portable solar charger and a solar rooftop array) were selected to show how various product integrations, usage durations, and disposal methods affect the possible environmental advantages of organic photovoltaics and to inform researchers about the opportunities for further advancement and expansion of this technology. With baseline cradle-to-grave impacts for both long-term uses (rooftop arrays) and short-term uses (portable chargers) on average 55% and 70% lower than silicon devices, respectively, the life-cycle assessment's findings demonstrated that the environmental benefits of organic photovoltaics go beyond the production of the panels. These findings show that additional savings can be achieved by incorporating organic photovoltaics into more straightforward devices that benefit from their adaptability and potential for use in less traditional technology-restricted applications. Organic solar charging units, for instance, demonstrated life-cycle impacts that were between 39 and 89 percent lower than those of silicon, as well as energy and carbon payback times that were as short as 220 and 118 days, respectively.

An approach known as life cycle assessment (LCA) was developed to assess the environmental effects of a single product at each stage of its life cycle. LCA can determine each contributor's share in different environmental impact profiles, including the materials and manufacturing processes used to create the product. Furthermore, a variety of PV technologies' environmental performance has been examined using this method extensively [Sherwani et al., 2010]. The most widely used indicators to differentiate the sustainability of a particular PV technology are cumulative energy demand (CED), GHG emission, energy payback time (EPBT), and GHG emission factor, among other life cycle impact categories used in prior LCA research in terms of PV technologies. When compared to other renewable energy technologies, PV technologies exhibit exceptional performance in terms of EPBT from an environmental perspective. Due to their dominant contribution—up to a 93% share in the PV market—monocrystalline silicon (mono-Si) and multicrystalline silicon (multi-Si) modules initially garnered more attention. The EPBTs of various silicon PV modules decreased from 3 to 4 years to 1 to 1.5 years due to technological advancements [Müller et al., 2021]. Then, in order to satisfy the need for flexible deployment, thin film PV technologies took center stage. Since the processes do not require the extraction of silicon material, amorphous silicon (a-Si:H), cadmium telluride (CdTe), and copper indium diselenide (CIS) were assessed with lower environmental impacts.

A cradle-to-grave life cycle assessment was used to compare third-generation organic and inorganic thin-film photovoltaics to a multicrystalline silicon module [Krebs-et al., 2021]. The effects of applying each type of panel to a photovoltaic system with a 3.6 GW capacity were computed. The silicon device is the current industry standard for solar energy, while the two thinfilm panels were selected as possible future directions for photovoltaic technology. In order to maintain the designated power capacity, panel installation was modeled linearly over a thirty-year period, accounting for replacements due to functional lifetime and efficiency degradation. To calculate the overall environmental impacts of meeting the AEDP target, the resulting environmental burdens were computed for each type of panel. By using life cycle assessment. In Ref. [Li, Q., Monticelli, C., & Zanelli, A. (2022)] examines the environmental performance of flexible organic solar cells and perovskite solar cells with GTEs. The detailed production procedures of GTEs are developed along with the solar cell manufacturing process. Two types of solar cells are covered by the thorough life cycle inventories (LCIs). LCIs claim that life cycle impact assessments are conducted in order to reveal different impact categories throughout their entire life cycles. The uncertainty of the ultimate environmental impacts is measured through sensitivity analyses that employ

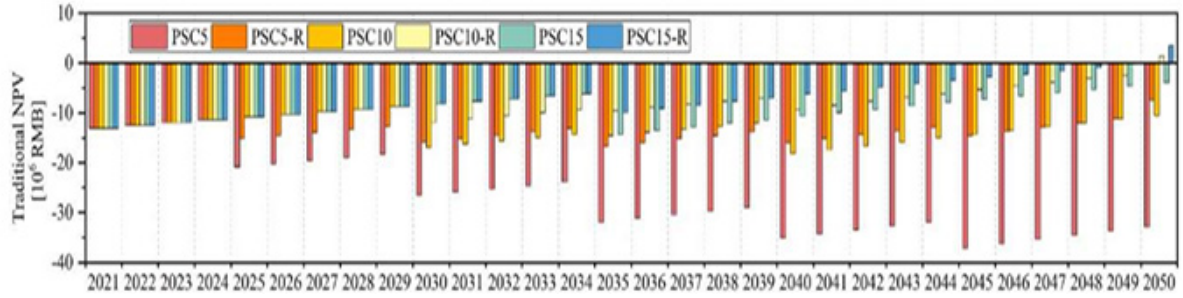
the Monte Carlo method. The findings demonstrate that the shortest Energy Payback Time is achieved by perovskite solar cells equipped with GTEs. Both solar cells should be made to last longer in order to satisfy the sustainable manufacturing requirement.

One of the most important stages of the life cycle assessment (LCA) study is the LCI. The Ecoinvent database contains all of the study's data. The ETFE material inventory is based on data provided by the Serge Ferrari Company. The PSC inventory is based on research by Gong et al. (2015), while the OSC inventory is based on research by A et al. (2017). An OPV solar park's lifecycle inventory was presented by Espinosa et al. in 2015. Additionally, [Espinosa et al. 2014] looked at various OPV life-cycle scenarios. A solar park with 960 m^2 of OPV modules, a lifespan of 15 years, and an EPBT of 0.88 years was the subject of one case study.[Roes et al. 2009] contrasted conventional Si-based PV technologies with OPV (polymer-based) cells. When compared to traditional PV technologies, the polymer-based configurations showed smaller environmental impacts (per Wp). The Cumulative Energy Demand (CED) associated with the production of small-molecule and polymer-based PVs is 50% lower than that of conventional inorganic PV technologies, according to [Anctil et al. 2013]. According to [Chatzisideris et al. 2017], OPV systems devoid of storage devices have the potential to reduce industrial carbon emissions. The effects of human toxicity and climate change are exacerbated by battery use. Additionally, [Chatzisideris et al. 2019] emphasized a few crucial elements that impact an OPV system's environmental profile. In a review of OPV, [Lizin et al.2013] reported EPBT values ranging from 0.29 to 0.52 years. The life-cycle environmental performance of solar chargers based on OPV technology was examined by [Glogic et al., 2019]. According to Hengevoss et al. [2016], compared to multi-Si or CdTe technologies, the production of a 1 m^2 tandem OPV module has a smaller environmental impact. OPV and other PV cell types were examined by Tsang et al. [2016]. In terms of EPBT, the default OPV configuration, the multi-Si option, and the amorphous silicon cells had respective results of 0.21, 2.7, and 2.2 years. There aren't many studies on OPV-ETFE systems, according to a review article [Lamnatou, C., Moreno, A., … D. C.-… and S. E., & 2018] about systems that combine OPV cells and ETFE [Lamnatou et al 2024].

In order to preserve the environment, [Li et al. 2025] create a process for recycling photovoltaic components. Given an initial budget constraint, multi-objective optimization is used to determine the best photovoltaic facade configuration. To confirm the efficacy of the suggested approach, a representative Central Business District building is chosen. The simulation is then expanded to include China's major cities. **Figure 13** shows the results of traditional NPV, which shed light on the building owner's financial gains or losses. Eighty percent of the PSC installation area is chosen to illustrate the conventional NPV trends. Since the installed PSC façade system has a capacity of about 3.0 M W, PSCs cost 4.33 RMB/W to buy. Three different PSC lifespans are included in the study: five years (PSC5), ten years (PSC10), and fifteen years (PSC15). The PSC5-R, PSC10-R, and PSC15-R recycling scenarios are also taken into consideration. The findings indicate that six PSC façade systems cost the same, 13.1 million RMB. All PSC façades fail to generate positive returns throughout their lifecycle if PSC recycling is not taken into account. PSC5, PSC10, and PSC15 have traditional net present values (NPVs) of −32.9M RMB, −10.5M RMB, and −3.9M RMB, respectively. Recycling PSCs can help investors reduce the façade's glare and increase the building owner's profit from PSC facades. With an impressive NPV performance of 3.5M RMB, PSC15-R stands out as the most financially sound of the six systems. Additionally, PSC10-R shows a net benefit of 1.4 million RMB. Nevertheless, PSC5-R continues to operate at a loss of 3.9 million RMB over its lifetime.

Because silicon PV panels have nonlinear output characteristics, the power output will be significantly reduced under partial shadow conditions [Li, Q., Zhu, L., Sun, Y., Lu, L., Energy, Y. Y.-, & 2020]. As a result, even though the vertical facade has a much larger area, silicon PV modules can only be used on the building's roof [An et al 2023]. Furthermore, because rigid and heavy flat PV modules increase envelope loads, they present difficulties for most building projects. PV module integration requires sturdy structures that can bear their weight, which frequently calls for reinforcing substructures like curtain walls. Accordingly, these modifications increase the cost of installation [Čurpek, J., Energy, M. Č.-R., & 2020]. High-rise building density and dense urban planning make it difficult to implement BIPV in urban areas.

Figure 13. Traditional NPV of Zhengda Center's PSC façade over a 30-year lifespan in Beijing.[Li, Q., Long, L., Li, X., Yang, G., Bian, C., Zhao, B., Chen, X., & Chen, B. M. (2025).



Semi-transparent photovoltaic (STPVs)

Photovoltaics, or (BIPV) and the increasing demand for development in the promotion of farmbased solar power, or agrivoltaics, the development of "Transparent Photovoltaics" (TPVs), or solar cells that are transparent to visible light, has gained popularity in recent years [Matsuki, N. (2023)]. Selective light-transmission photovoltaics (SLTPVs), which let some incident light escape to the back, have already been used in practice. These devices use conventional bulk and thin-film solar cells that are fabricated into long, thin strips and arranged like a window shade at intervals or by reducing the film thickness. However, because SLTPVs block the view outside the window and keep enough light from reaching the interior or farmland surface, their installation applications are limited. It is anticipated that the range of applications will greatly increase if TPVs that are tintedtransparent, like window glasses or uniformly transparent, can be made commercially available.

Humans consider TPVs to be "nearly colourless" if their visible light transmittance, including the substrate material, is 80% or higher. Red and dark colours can be produced by adjusting, depending on the application.Due to their capacity to lower CO_2 emissions through "window power generation" in fully glazed buildings (building-integrated material characteristics that allow for uniform absorption of either the long wavelength side of the visible light wavelength range, the short wavelength side, or the entire wavelength range) [Matsuki, N. (2023)]. Semitransparent photovoltaics (STPVs) are solar cells that transmit visible light and have a visible light transmittance of 80% or less. Because of their satisfactory transparency and solar power generation, semi-transparent photovoltaics (STPVs) are an economical, efficient, and environmentally friendly technology that has been used in building integrated photovoltaics (BIPV) [[Wu, Z., Zhang, L., Wu, J., Energy, Z. L.-, & 2022]]. Because of their high tolerance to changes in light angle and intensity, tunable colour, and adjustable transparency, dye-sensitised solar cells (DSCs) have emerged as promising candidates for STPVs [Zhou, H., Energy, H. K.-M. T., & 2023]. Because of their high transmittance in the 600–700 nm range, semi-transparent DSCs in agrivoltaics, in particular, ensure photosynthesis and seed germination in addition to producing electricity [[Yang, et al 2022]]. A problem in the DSC application process is that semi-transparent DSCs have not yet been able to concurrently satisfy the needs of appropriate transmittance, high efficiency, and exceptional stability.

Every component of the device should be optimised to produce the perfect semi-transparent DSCs. For instance, the transmittance of DSCs can be improved by decreasing light scattering and increasing the electrode material's dispersion [[Wu, C., Li, R., Wang, Y., Lu, S., Lin, J., ... Y. L.C., & 2020]]. The development of high-performance semi-transparent DSCs is greatly impacted by the electrolyte, a crucial component of DSCs that has a major impact on ion diffusion and device stability. Optimising the diffusion behavior of redox couples in gel polymer electrolyte (GPE) is therefore crucial. By decreasing crystallinity, copolymerization, the addition of nanofillers, and polymer blending can encourage ion diffusion in GPEs [[Venkatesan, S., Chen, Y., Chien, C., ... M. T.-J. of I. and, & 2022].

STPVs can demonstrate both high power conversion efficiency (PCE) and average visible transmittance (AVT) by varying the absorption of visible light. While the maximum PCE for an opaque cell is 33%, Lunt (2012) reported that the maximum PCE for a highly transparent STPV (70% AVT) was approximately 24%. With band selective (BS) absorption of specific visible wavelengths, the maximum PCE for STPVs with the same transparency can actually surpass this limit, reaching 28%. Additionally, the maximum light utilization efficiency (LUE) is raised from 20% to 23% using this BS method. In addition to performance limitations, research on harvestable irradiance for STPVs in urban settings is necessary for precise power output forecasts, but these studies are not frequently available. In order to derive empirical spectra for both sunny and cloudy conditions, [Wong, V. K., Ho, J. K. W., Wong, W. W. H., & So, S. K. (2025)] examined solar irradiance in 16 cities over a ten-year period. Infrared (IR) makes up 85–90% of invisible irradiance, and the maximum harvestable irradiance for fully transparent PVs in cities is ~460 W/m^2 in clear skies and ~50 W/m^2 in overcast conditions, which is different from the AM 1.5G standard (~570 W/m^2). Depending on the transparency of the absorber, the corresponding maximum output power intensity varies between 150 and 250 W/m^2 (sunny). According to our research, organic materials with high AVT and IR bandgaps (0.9–1.4 eV) are perfect for highperformance STPVs. Functional layer analysis reveals that certain encapsulants and charge extraction layers can hinder PCE by obstructing invisible light, and metal electrodes may limit overall transparency unless they are thinned or nanopatterned. These findings provide thorough recommendations for material scientists and energy researchers looking to optimize and analyze STPVs.

Due to the uneven spectral transmittance in the visible wavelength region, the majority of STPV devices are not color-neutral [Kumar, P., You, S., & Vomiero, A. (2023)]. Therefore, when targeting BIPV applications like glass windows, another parameter to take into account is the color perception (aesthetics) of semitransparent solar cells in addition to PCE and transmittance. The industry standard for measuring the color that the human eye perceives from a measured spectrum is the International Lighting Commission's (CIE) 1931 (x, y) chromaticity diagram. In the work of [Fihn, M., Chen, J., & Cranton, W. (2011)] The standard solar spectrum used to characterize the PCE (AM 1.5G) has color coordinates

of (0.3202, 0.3324), and the so-called "white point" or neutral color corresponds to coordinates of (0.3333, 0.3333). [Z Hu and others, 2020] As an alternative, the CIELab color space can be used to report chromaticity coordinates with three parameters: a*, b*, and L.[Buildings, B. J.-E., Røyset, A., Kolås, T., & 2020] Additionally, color comfort and aesthetics are crucial. As a result, other figures of merit are assessed, including correlated color temperature (CCT) and color rendering index (CRI).Roy, A., Sundaram, S., Selvaraj, P., Bhandari, S., Ghosh, A., & Mallick, T. K. (2019)] A high CRI value (near 100) indicates that there is minimal color variation between the original reference light and the light that is transmitted through the solar cells. In addition, color temperature is a measurement of how bluish (cool) or yellowish (warm) a color appears; warm colors have a color temperature between 2700 and 3000 K, while cool colors have a color temperature above 5000 K.

Currently, using photovoltaics to power buildings is becoming more and more important due to the increased energy consumption of buildings [Ahmed, W., & Asif, M. (2020)]. According to a techno-economic analysis conducted by Imam et al. (2019), a typical Saudi apartment requires a minimum of 12.25 kW of grid-connected photovoltaics.The feasibility of constructing rooftop solar systems for Saudi Arabian architecture, which hardly ever uses PVSDs, was investigated by Lopez-Ruiz et al. in 2020. Only a small number of studies have looked at the vertical and horizontal photovoltaic shading devices in terms of insolation [Sustainability, O. A.-, & 2018] or the overall energy performance of external fixed PVSDs over conventional shading devices [Mesloub, A., & Ghosh, A. (2020)]. Thus, the College of Engineering building of the University of Ha'il, which is situated in a hot desert, served as the case study reference office building (ROB) for this study's case study of the overall energy performance and visual comfort of five distinct configurations. Solar gains, daylighting, and the ROB's HVAC system were all modeled using the EnergyPlusTM program [Oh, S., Hildreth, A., Oh, S., Energy, A. H.-A. for S., & 2016] and the DIVA-for-Rhino© software plug-in [Mohsenin, M., & Hu, J. (2015)] along with the energy generated as a result of PVSD integration. Experimental research using an off-grid system was used to analyze the maximum energy output of solar PVs tilted at different angles and degrees. Lastly, the ROB, a typical office building in Saudi Arabia, was compared to the prototype small offices retrofitted with each of the five configurations to determine how much energy they could save.

Used Energy-plus and DIVA-for-Rhino© plug-in building energy simulation tools to investigate for the first time the effects of retrofitting four distinct PVSD configurations and one STPV module to a south-facing prototype small office model in the University of Ha'il's College of Engineering building, under a hot desert climate, on overall energy performance and visual comfort. To identify the ideal tilt angle, 30°, and to confirm the results of our simulation models, a thorough examination of the annual and hourly energy output of different tilt angles was first carried out using an off-grid system. To achieve maximum energy output, a 30° tilt was incorporated into the design of the tilted five-slat louvre, tilted ten-slat louvre, and inclined single panel PVSDs. Finding the ideal configuration requires striking a careful balance between energy efficiency and visual comfort [Matsuki, N. (2023)]. Our simulations' outcomes brought to light the following crucial points. The integration of outward tilted slats in the louvre PVSDs and the double-low-E window pane of the STPV module greatly decreased cooling and heating energy consumption because of the thermal properties of the STPV window pane in comparison to double-low-E window panes applied in other configurations. This indicates that climate had a significant impact on cooling and heating energy consumption. Additionally, it provided yearround protection from direct solar radiation.

- Even though glare discomfort could be eliminated with a good configuration and daylight control strategy, they increased lighting energy consumption, especially in the STPV module.
- The unfilled eggcrate PVSD was the best setup since it could provide visual comfort and generate more energy with a conversion efficiency of - = 20%.

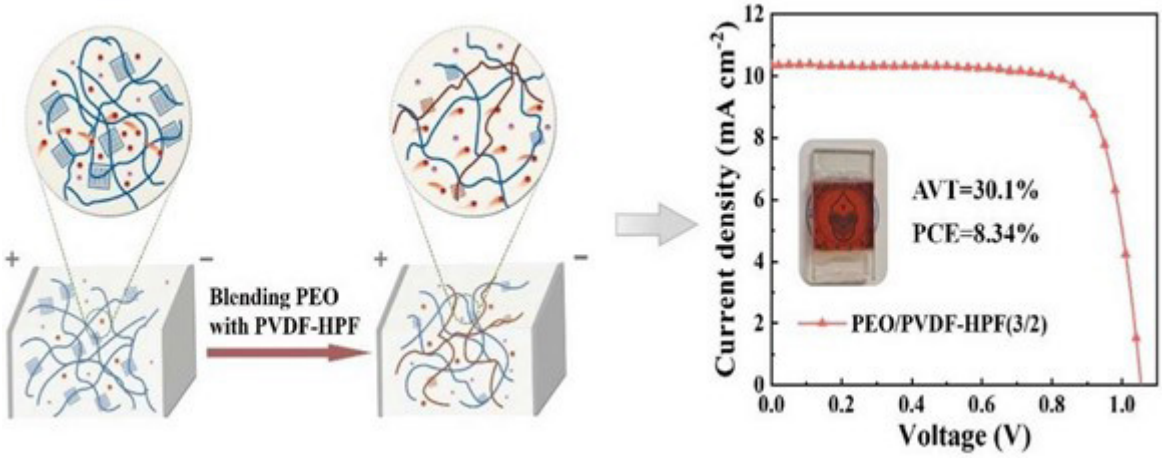
Incorporating STPV modules and PVSD systems into the building envelope improves visual comfort, reduces CO_2 emissions, and offers significant energy savings potential that could exceed zero net energy consumption [Matsuki, N. (2023)].

(PVDF-HPF) gel polymer electrolyte of semi-transparent dye-sensitized solar cells

A crucial first step in the commercialization of semitransparent photovoltaic technologies is the development of large-area semitransparent solar modules. However, it has not yet profited from the substantial scientific advancements in the field of perovskite solar cells, most likely because of the challenges in producing a large-scale, highly uniform, semitransparent light absorber [Shi et al., 2025] suggested combining poly (ethylene oxide) (PEO), a conventional commercial polymer, with poly (vinylidene fluoride-co-hexafluoro propylene) (PVDF-HPF) in order to improve D_{app} and decrease crystallinity. Compared to the GPE prepared with PEO, which achieved a high efficiency of 8.34% in DSCs, the D_{app} of GPE obtained at the ideal ratio of 3/2 was twice as high. Semi-transparent DSCs with an average visible light transmittance (AVT) of 30.1% were produced by combining this with a thin photoanode that had been sensitized by Y123. Additionally, by giving mung bean seedlings ideal growing conditions, the semi-transparent DSCs demonstrated agrivoltaic applications. Our research served as a guide for

the development of high-performance semi-transparent DSCs in addition to proving that the polymer blending approach was appropriate for encouraging the diffusion of large-size Cu redox couples in GPE. When paired with a 1.2 μm photoanode, a 30.1% AVT was achieved. By preventing the regular arrangement of polymer chains and decreasing crystallinity, **Figure.14** tried the polymer blending strategy to encourage the diffusion of large-size $Cu^{I/II}(tmby)_2$ in GPE.

Figure 14. PEO/PVDF-HPF gel polymer electrolyte of semi-transparent dye-sensitized solar cells with high performance based on Cu [Shi, et al 2025].



A semitransparent solar module with a uniform semitransparent absorber with a large area of 40.8 cm^2 and a geometrical fill factor of 95.6% is reported. It is made of a vertically aligned onedimensional nanopillar $CH_3NH_3PbI_{3-x}Cl_x$ perovskite that was created using an anodized aluminum oxide (AAO) template. Reduced light reflection and the development of a uniform perovskite morphology are made possible by the AAO scaffold. Because of the limited carrier path, the uniform nanopillar-structured perovskite-based device shows improved electrical properties. With a power conversion efficiency of 9.04% and an average visible-light transmittance of 30.2%, this optimized nanopillar-based semitransparent solar module with nine sub-cells [Kwon et al., 2020] clearly shows promise for real-world power-generating window applications. Several synergistic techniques are used by [Rai et al. (2021)] to guarantee high transparency while enhancing the ST perovskite film's stability and quality. It has been discovered that doping the perovskite with europium ions suppresses the production of harmful species such as elemental Pb and I, increasing atmospheric stability. The top transparent contact's effect is intended to produce a green hue and an average visible transparency (AVT) of greater than 20% for the entire device. Finally, the use of a down-converting phosphor material, which captures low energy photons and prevents UV-induced degradation, enhances the lower current density brought about by the thinner ST absorber. In 21 cm^2 ST-PSM, this multimodal approach produces a power conversion efficiency of 9.5% under one sun's illumination and 12% under dim light In Ref. [Sun and others, 2023] uses sandwich-structure silver nanowires to create a transparent top electrode that can be processed in a solution, achieving high transparency in semi-transparent organic solar cells. A modified hole-transport layer called HP enhances the electrode's wettability and conducting capabilities. With an average visible transmittance of 50.8%, a power conversion efficiency of 7.34%, and the highest light utilization efficiency of 3.73% in the absence of optical modulations, the semi-transparent solar cell demonstrates good see-through qualities. Furthermore, when compared to their Ag electrode counterparts, flexible devices built using the aforementioned architecture exhibit superior mechanical tolerance, maintaining 94.5% of their initial efficiency after 1500 bending cycles. [Li and others, 2021] An infrared absorbing nonfullerene acceptor, or H_3, is chosen from a wide range of photo-active materials using a numerical method developed to measure the absorbing selectivity of materials and devices. Second, polyethylenimine wetting is used to create an ultra-smooth transparent thin Ag layer with tiny granules, which reduces light scattering and enhances the electric characteristics for ST-OPV. To further enhance the light-absorbing selectivity, a TeO_2 capping layer is deposited on top of the ultra-thin Ag under the guidance of optical simulation. This results in a good color rendering index of 76.85 and a significant improvement in light utilization efficiency to 3.95 ± 0.02% (best ≈4.06%). It is among the best color-neutral ST-OPVs because of these outcomes.

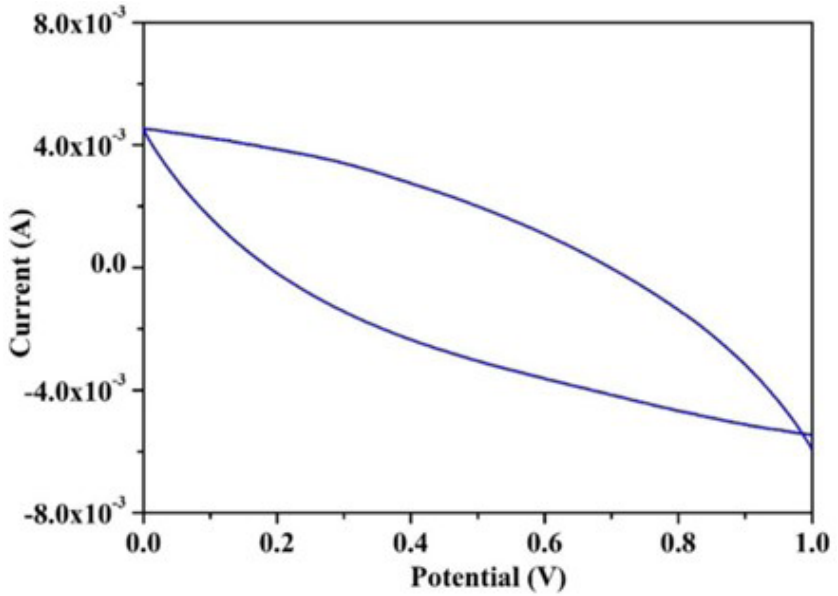
In the work of [Chang and others, 2020] for the first time, we created ST-OSCs based on the PM6:N_3 active layer using the MoO_3-/Ag-/MoO_3-based D/M/D transparent electrode. By altering the outer MoO_3 layer's thickness during device fabrication, the D/M/D transparent electrode was optimized. Consequently, we discovered that while thickening the outer MoO_3 layer can raise the device's average visible transmittance (AVT), it can also lower its power conversion efficiency (PCE).

With a high AVT of 28.94% and a PCE of 9.18%, the outer MoO_3 layer with a thickness of 10 nm was determined to be the ideal scenario. With a high color rendering index (CRI) of over 90 and a neutral color perception, all semi-transparent devices demonstrated significant promise.

The development and performance analysis of a supercapacitor employing polyethylene oxide (PEO)-derived activated carbon as the electrode material and a solution-cast polymer electrolyte based on poly(vinylidene fluoride-co-hexafluoropropylene) (PVdF-HFP) for dye-sensitized solar cell (DSSC) application are investigated by [Nazir et al., 2025]. This paper discusses polyetherbased electrochemical devices, in which PVdF-HFP is used to prepare an electrolyte and polyethylene oxide (PEO) is used to develop the electrode material. The results of extensive electrical and photoelectrochemical investigations using a variety of characterization techniques are thoroughly examined. The maximum conducting polymer electrolyte used in sandwich structure supercapacitors and DSSCs has an ionic conductivity of 8.3×10^{-5} Scm^{-1}, a high specific capacitance of 395 Fg^{-1}, and a DSSC efficiency that ranges from 1.6 to 3.5% under one sun condition. Corn starch is used as a base biopolymer to create ionic liquid biopolymer electrolyte (ILBPE), a vital component of advanced energy storage and conversion devices like dye-sensitized solar cells (DSSC) and electric double-layer capacitors (EDLC). Alongside biopolymers, ionic liquids—like the stable compound 1-ethyl-3-methylimidazolium tricyanomethanide—are used to increase ion mobility at temperatures lower than 100 °C [[Jothi, et al 2021]], which is crucial for enhancing the functionality of electrochemical devices. Devices like electric double-layer capacitors (EDLCs), which are renowned for providing noticeably higher capacitance than conventional dielectric capacitors [Jothi, M., Vanitha, D., ... K. S.-I. J. of, & 2022], depend on this increased mobility to function properly.

Solution casting is used to create proton conducting solid polymer electrolyte [SPE] based on cornstarch [CS] and polyvinylpyrrolidone [PVP] with ammonium acetate. AC impedance techniques can be used to determine the conductivity and dielectric of this proton conducting SPE. At room temperature, sample AA-60 exhibits a higher conductivity of 1.09×10^{-6} S/cm with an activation energy of 0.403 eV. The conduction mechanism of overlapping large polaron tunneling (OLPT) is followed by higher conducting SPE. The maximum transference number (approximately 0.99), as determined by the transference number analysis, is 60 weight percent. The cation has a higher mobility and diffusion coefficient (D) than the anion.The applied potential window of -0.2 to 0.7 V is where the recorded CV curve is located. The manufactured proton battery has achieved a discharge time of 63 hours and an open circuit voltage of 0.89 V[Jothi and others, 2022]. Using corn starch, potassium iodide (SSKI oral solution), and the organic ionic liquid 1-Ethyl-3-methylimidazolium Tricyanomethanide (EmImTCM) via the solution cast technique, [Konwar et al. 2025] have successfully created a high-conducting biopolymer electrolyte. Our method is unique in that it incorporates this ionic liquid into the biopolymer matrix, which improves the electrolyte's thermal and electrochemical stability while also increasing ionic conductivity. The capacitive nature and specific capacitance of the EDLC cell are investigated using cyclic voltammetry (CV). Because of the ion's mobility towards the porous carbon electrode, which forms the Helmholtz layer in either electrode of the EDLC and causes the non-faradic process of electrode polarization, the CV plot shown in **Figure 15** resembles a rectangular shape, which is seen in the case of EDLC.At one sun condition, the DSSC has an efficiency of 1.44%, while the fabric electrochemical device EDLC has achieved an average specific capacitance of up to 200F/g.

Figure 15. The manufactured EDLC cell's cyclic voltammetry profile at 10 mV/s in the voltage range of 0 V to 1 V. [Konwar, et al 2025]

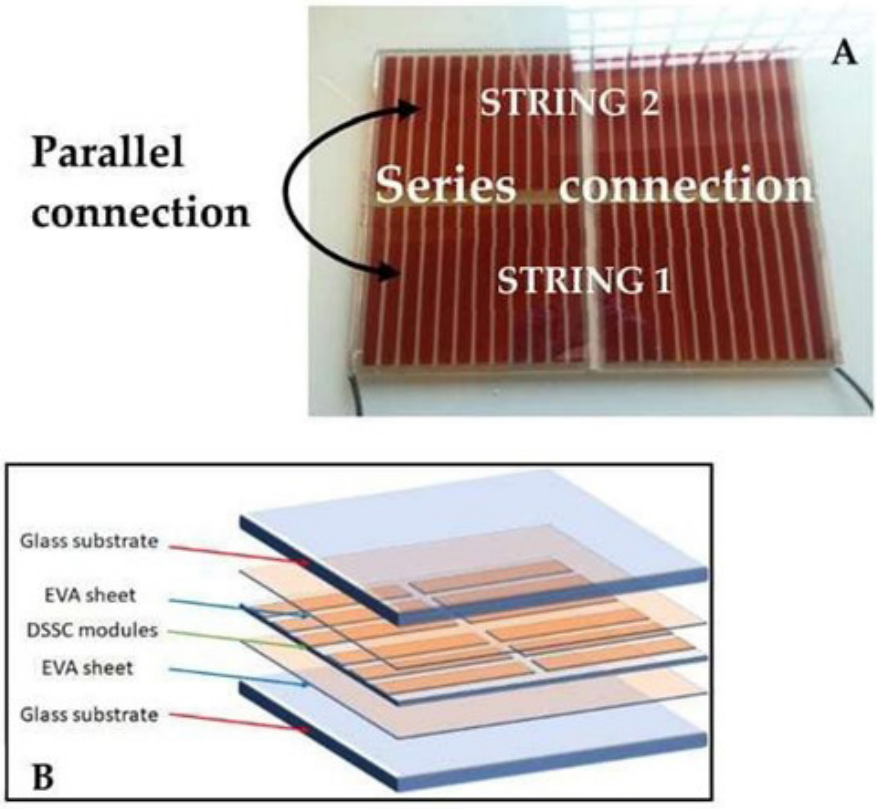


SEMI-TRANSPARENT DSCS DEMONSTRATED AGRI-VOLTAIC APPLICATION

The world's population is still increasing, and with it, so is the demand for food. In order to combat climate change and global warming, areas will be used to produce clean electricity concurrently. "Agrivoltaic technology," which combines solar photovoltaics and crop production, offers benefits to both parties and offers a sufficient, resource-efficient solution to the ongoing issue of competition for arable lands. From the initial capacity of 5 MW in 2012, the deployment of agrivoltaic systems has grown rapidly in recent years, reaching the global installed capacity of 2.8 GW in 2020. The majority of agrivoltaic systems installed globally use traditional opaque photovoltaic (PV) modules, which alter the microclimate beneath the panels and become problematic at high shading ratios. The use of semi-transparent technologies based on crystalline silicon (c-Si), thin-film photovoltaic, organic PVs (OPVs), dye-sensitised solar cells (DSSCs), concentrating PVs (CPVs), and luminescent solar concentrators (LSCs) in open (arable farming lands) and closed (cultivation greenhouses) agrivoltaic systems has been used recently to mitigate this issue, which is thoroughly examined in this research [Gorjianet al 2022]. The findings showed that, when compared to other technologies, c-Si STPV modules have the highest employment share in agrivoltaic systems because of their extreme advantages: low costs, high stability, and high efficiency. In contrast, thin-film STPV modules have hardly been documented in the literature.

One of the most interesting technologies is photovoltaic (PV) [Barichello et al., 2021]. Innovative photovoltaic devices, dye-sensitised solar cells (DSSCS) are renowned for their promising qualities of colour tenability, low cost, and ease of fabrication. Given their dual function of filtering light and meeting energy needs, all of these characteristics make DSSC technology appropriate for application in the so-called agrovoltaic field. Utilised 40 DSSC Z-series connected modules to test the devices in a greenhouse while combining their high conversion efficiency, transparency, and robustness. The module's aperture (312.9 cm^2) had a 35% transparency, resulting in a maximum conversion efficiency of 3.9% on a 221 cm^2 active area. Additionally, various modules demonstrated robust stability for 1000 hours when stressed at two different temperatures (60 °C and 85 °C) and under light soaking at the maximum power point and put the manufactured modules together to create ten panels that would filter the greenhouse's roof light. Each string was made up of two serially connected modules with similar currents to prevent any performance drops (**Figure 16a**). An industrial laminator (Laminator Core 2, Rise Technology srl) was used to laminate two strings into a panel using a hot vacuum lamination process. To minimize stress on the DSSC modules and stop electrolyte leakage, a low-temperature strategy (max temperature of 85 °C) was created and implemented. Two 450 µm-thick low-temperature cross-linking EVA sheets served as encapsulants, while two 4 mm thick tempered glasses served as external substrates [see **Figure 16(b)**].

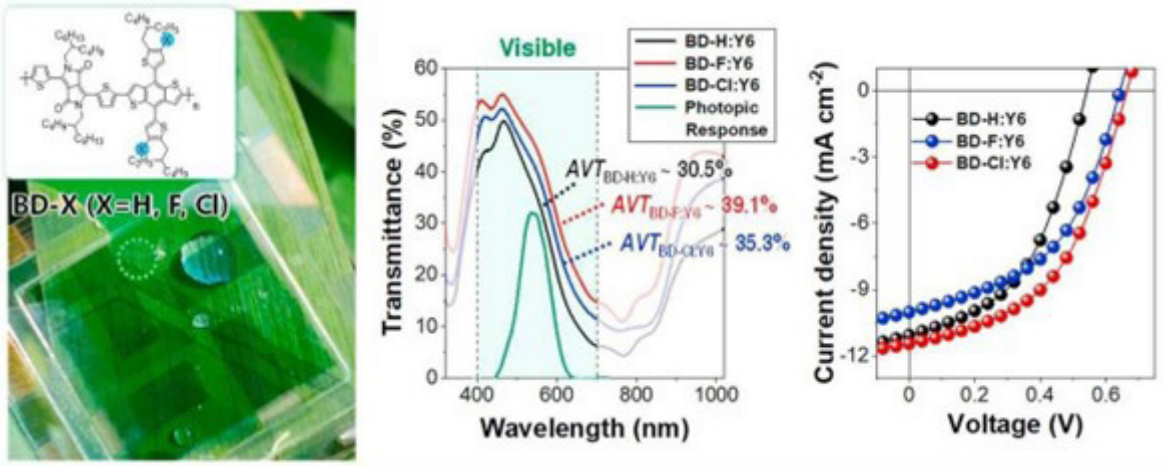
Figure 16. The 4 × 4 DSSC panel (A) is made up of two serially connected DSSC strings arranged in parallel; the DSSC panel structure (B). [Barichello et al 2021].



In Ref. [Jinnai and others, 2023] It is suggested to use green-light wavelength-selective OSCs, whose blue and red light can be efficiently utilised to stimulate plant growth. To create green-light wavelength-selective OSCs, naphthobisthiadiazole-based compounds (SNTz-RD and ONTz-RD) are newly designed as acceptors, and a useful polymer of poly (3-hexylthiophene) (P3HT) is used as the donor. Strong absorption bands are visible in the green-light region of the SNTz-RD and ONTz-RD electronic absorption measurements. Furthermore, as acceptors, SNTz-RD and ONTzRD have the proper frontier orbital energy levels. With good green-light wavelength-selective factors and good power conversion efficiencies in the green-light region, OSCs based on P3HT and these acceptors exhibit typical photovoltaic responses. Furthermore, when compared to the traditional P3HT: [6, 6]-phenyl-C61-butyric acid methyl ester (PC61BM) film, the P3HT:SNTzRD blend films show an enhanced photosynthetic rate in the strawberry leaves. These findings show that green-light wavelength-selective OSCs for use in new greenhouse agrivoltaics can be created by combining P3HT with green-light wavelength-selective acceptors .TB7-Th and DPPbased polymer donors are popular delegations for ST-OSCs in polymer donors that preferentially absorb long wavelengths [Wang, Y., Wang, G., Xing, Y., ... M. A.-M. C., & 2021].

Due to their high transmittance in the visible region, DPP-based polymer donors exhibit strong light absorption between 600 and 900 nm, suggesting that they are appropriate materials for the photoactive layers of ST-OSCs [Xue et al., 2021]. Furthermore, the electron-deficient DPP unit exhibits strong π-π stacking due to its planar conjugated structure from a material standpoint. Furthermore, in order to achieve effective charge transport properties and a narrow bandgap, the thiophene unit next to the DPP reduces steric repulsion with the DPP while preserving the coplanarity of the polymer backbone [Lee et al., 2012]. A DPP-based polymer has been used to fabricate ST-OSCs with a performance of up to 13.21% based on the previously mentioned characteristics, which results in high transmittance and efficiency simultaneously [Rasool, et al 2022]. Halogenation techniques were used to create high transmittance ST-OSCs with increased efficiency [Park et al., 2023]. For the polymer donor, we chose the DPP unit as the acceptor and the BDT unit as the donor. We created three polymer donors and called them BD-H, BD-F, and BD-Cl, respectively, after adding H, F, and Cl to the BDT side chain. In addition to fine-tuning the polymer's morphology and crystallinity, fetching tactics would also downshift the HOMO. As a result, the power conversion efficiency (PCE) of the BD-Cl:Y6 OSCs was 5.62%. Additionally, the BD-Cl:Y6 ST-OSC showed a high average visible transmittance of 35.1% and PCE of 3.69% after a metal oxide/metal/metal oxide transparent electrode was added. The potential of ST-OSCs is increased by this method in **Figure 17**.

Figure 17. Creation of a halogenated low bandgap polymeric donor for organic solar cells that are semi-transparent and near-infrared [Park, et al (2023)].

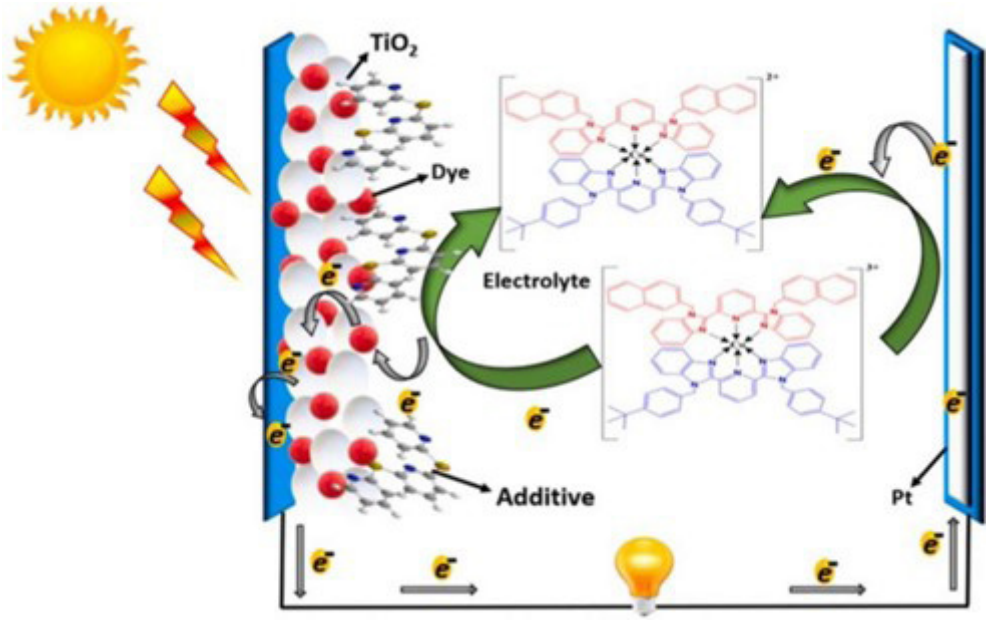


ORGANIC GEL POLYMER ELECTROLYTE FOR SOLAR CELL

Leakage or evaporation of the liquid electrolyte limits the DSSCs' long-term durability. As a result, attempts have been made to substitute a polymer electrolyte, molten salt, inorganic p-type semiconductors, or organic hole transport materials for the liquid electrolyte [Rahman et al., 2004]. The polymer has a major impact on the electrolyte's PCE in DSSCs based on gel electrolytes. Polyacrylonitrile, poly(acrylic acid), poly(ethylene glycol), polypyrrole, poly(poly(acrylic acid)co-ethylene glycol), and poly(vinylidene fluoride-co-hexafluoropropylene) are among the numerous polymers that have been employed as gelators or as a medium to transport redox shuttles thus far [Ileperuma, O. A., Asoka Kumara, G. R., Yang, H.-S., & Murakami, K. 2011]]. For polymer gel electrolytes, these polymers are typically combined with commercial organic additives and the I−/I3− redox shuttle.

In Ref. [Balamurugan, S., Ganesan, S., Kamaraj, S., Mathew, V., Kim, J., Arumugam, N., & Almansour, A. I. (2022)] [2,6-bis (1-(4-(tert-butyl)benzyl)-1H-benzo[d] imidazole-2-yl)pyridine] is a recently developed heteroleptic cobalt I/II.To improve the power conversion efficiency (PCE) of dye-sensitised solar cells (DSSCs), pyridine-based organic additive 2, 6-bis(pyridin-2ylthio) pyridine (BPTP) and 1H-benzo [d] imidazole-2-yl)pyridine)] redox shuttle ($Co2^{+}/3^{+}$[(bnbip) (b(tbb)bip)]) were first added to the Poly(ethylene glycol) gel polymer electrolyte. Under 1 sun (100 mW/cm^2) conditions, the PCE of the device with PEG/ $Co2^{+}/3^{+}$[(bnbip) (b(tbb)bip)]/BPTP gel electrolyte reached up to 5.12%, which was better than the device with PEG gel polymer electrolyte without BPTP. Longer electron life time (1.3 ms), lower charge transfer resistance (217 Ω), lower charge transfer kinetics (0.77 ms^{-1}), higher chemical capacitance (5.99 × 10^{-3} F), high diffusion coefficient (2.59 × 10^{-5} cm^2 s^{-1}), and a shift in the Quasi Fermi level of TiO_2 were some of the effects that confirmed this PCE enhancement. Recombination between TiO_2 and Co_3^{+} species of the Cobalt redox pair is easily suppressed by the recently integrated $Co_2^{+}/3^{+}$[(bnbip) (b(tbb)bip)] redox and BPTP additive in PEG gel polymer electrolytes in **Figure 18**.

Figure 18. Impact of poly (ethylene glycol) gel polymer electrolyte with pyridine-based organic additive and new heteroleptic cobalt redox shuttle on dye-sensitized solar cell performance [Balamurugan, S., Ganesan, S., Kamaraj, S., Mathew, V., Kim, J., Arumugam, N., & Almansour, A. I. (2022)].

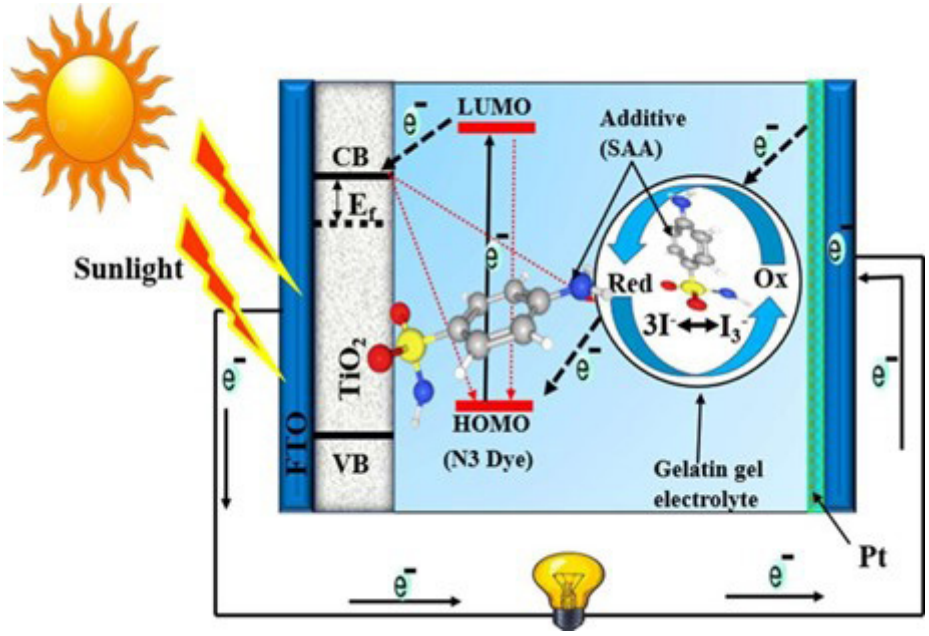


N-methyl pyridine iodide, a novel organic iodide salt, was synthesized by [Wu et al. 2006]. A gel polymer electrolyte was made using the N-methyl pyridine iodide as the I-source and poly (acrylonitrile-co-styrene) as the polymer matrix. N-methyl pyridine iodide is a type of organic iodide salt, which means that it dissolves more readily in organic solvents than alkaline iodide compounds. However, because of its large cation, N-methyl pyridine iodide is easily separated from the molecule. Consequently, a comparatively high conductivity will be achieved by the gel polymer electrolyte that contains the novel iodide salt. The performance of dye-sensitized quasisolid-state solar cells made with a gel polymer electrolyte will be comparatively good. A porous membrane is soaked in an organic electrolyte solution that contains the $I3^{-}/I^{-}$ redox pair to create a gel polymer electrolyte. At room temperature, the gel polymer electrolyte has an ionic conductivity of 2.7 × 10^{-3} S cm^{-1}, and it effectively encapsulates the electrolyte solution without allowing solvent leakage. At an incident light intensity of 100 mW cm^{-2}, a dye-sensitized solar cell (DSSC) using the gel polymer electrolyte produces an open-circuit voltage of 0.72 V and a short-circuit current of 6.27 mA cm^{-2}. This results in a 2.4% conversion efficiency. Compared to a DSSC assembled with a liquid electrolyte, the DSSC using the gel polymer electrolyte exhibits more stable photovoltaic performance [Kim et al., 2005].

In the work of [Abisharani et al 2021] The KI/I_2 redox pair and low-cost organic additives were used to create a novel series of GLN gel polymer electrolytes. For the application of DSSCs, five different organic compounds containing N, O, and S were employed as additives. According to EIS analysis, compared to other organic additives, the conductivity of the SAA organic additive integrated gel polymer electrolyte increases by up to 2.93X10^{-5} S/cm. In order to clarify the charge transport mechanisms at the interface between the photo electrodes and the electrolyte medium of the devices, the EIS experiment reveals the interfacial study in DSSCs. The charge transfer studies reveal that the SAA integrated GLN gel polymer electrolyte has a lower Rpt (685 Ω), higher Rct (1674 Ω), and Cμ (5.702 X 10^{-6}F) values. This establishes a shift to the Fermi level of TiO_2 and validates the mitigation of the recombination

process between TiO_2 and I3-ions. The strength and mode of interaction of each additive adsorbed on TiO_2 surfaces are also confirmed by DFT calculations. Under 100mWcm^{-2} of sunlight, the PCE is improved by up to 5.8% thanks to the N, O, and S in the SAA additive with GLN gel polymer electrolyte. **Figure 19**.

Figure 19. Using organic additives in gelatin gel polymer electrolyte for dye-sensitized solar cells that contain electron-rich donors (N, O, and S) [J.M. Abisharani et al 2021][Abisharani, J. M., Balamurugan, S., Thomas, A., Devikala, S., Arthanareeswari, M., Ganesan, S., & Prakash, M. (2021)].



The M^+ is a cation in the alkaline series Li^-Cs. Gel polymer electrolytes of general formulation polyacrylonitrile (PAN)/ ethylene carbonate (EC)/propylene carbonate (PC)/MI were prepared and employed in DSSCs. In order to construct DSSCs using the gel electrolytes, photo-anodes were made by adsorbing organic sensitizer D35 on nanocrystalline TiO_2 thin films. The results of nanosecond transient spectroscopy showed that the presence of large cations (Cs^+, Rb^+) sped up the dye regeneration process a little. Furthermore, Mott–Schottky analysis revealed a negative shift in the TiO_2 flat-band potential as the cations' charge density decreased (increasing size). Overall, the results show that photocurrent values, which in turn depend on the conductivity increasing with cation size, largely control cell efficiencies [Bettucci et al., 2018]. Poly (oxyethylene) diamine (POE-amine) and an aromatic anhydride were used to create a cross-linked copolymer, which was then cured to produce an amide-imide cross-linking structure. The copolymer's ability to absorb liquid electrolytes in methoxypropionitrile (MPN) for appropriate applications in dye-sensitized solar cells is due to its multiple chemical groups, including POE, amido acids, and imide. The same copolymer was investigated using various electrolyte solvents, such as propylene carbonate (PC), dimethylformamide, and N-methyl-2-pyrrolidone, in order to demonstrate the benefits of polymer gel electrolytes (PGE). [Shen et al. (2014)] demonstrated the copolymer's long-term stability. Field emission-scanning electron microscopy demonstrated that the copolymer's morphology after absorbing liquid electrolytes in these solvents was identical to that of threedimensional interconnected nanochannels. PC was chosen as the optimal PGE among these solvents because it showed a higher power conversion efficiency (8.31%) than the liquid electrolyte (7.89%).

In addition to electrolytes, dye is an essential part of a DSSC. In order to capture sunlight and transform it into electrical energy, the dye is essential. In DSSCs, ruthenium complexes show high energy conversion efficiencies and are efficient sensitizers [Shi et al., 2010]. Nevertheless, these dyes contain complexes of Ru metal compounds, which are costly and pollute the environment [Chang et al., 2010]. Another strategy is to use natural dyes made from fruits, flowers, and plant leaves, which are readily available, inexpensive, easy to prepare, and environmentally friendly. However, there are currently no suitable natural dyes that can provide high efficiencies. Anthocyanin derived from various natural sources has been used as the natural dye sensitizer in the majority of the work documented in the literature on natural dye-based DSSCs because it is anticipated to have good binding with the TiO_2 surface [Yuliarto et al., 2010]. The other common dye is chlorophyll. References [Ruhane, et al. (2017)] and [Zhou, H., Wu, L., Gao, Y., & Ma, T. (2011)] provide good reviews of the different natural dyes used for DSSCs.

In Ref. [Noor and others, 2014] DSSCs with natural dye sensitizers were created using a plasticized polymer electrolyte

system made of PVDF-HFP, sodium iodide (NaI), and an equal weight of ethylene carbonate (EC) and propylene carbonate (PC) as the binary plasticizer. Because of their favorable and promising characteristics for ionic conduction in polymer electrolytes, such as their low viscosity and high dielectric constant, ethylene carbonate (EC) and propylene carbonate (PC) were selected as plasticizers. The polymer electrolyte with 48 weight percent PVDF-HFP, 32 weight percent NaI, and 20 weight percent EC/PC has the highest room temperature conductivity, measuring 1.53×10^{-4} S cm^{-1}. A DSSC with the configuration FTO/TiO_2/natural dye/electrolyte/Pt/FTO has been fabricated using this electrolyte. With a shortcircuit current density of 2.63 mA cm^{-2}, an open-circuit voltage of 0.47 V, a fill factor of 0.58, and the highest photo-conversion efficiency of 0.72% when exposed to 100 mW cm^{-2} of white light, the dye mixture-containing DSSC performs the best. The fill factor improved from 0.58 to 0.59 and 0.60 and the photo-conversion efficiency rose from 0.72% to 1.11% and 1.85%, respectively, under illumination of lower light intensity of 60 mW cm^{-2} and 30 mW cm^{-2}.

CHALLENGES

Even though DSSCs are expected to be at least five times less expensive than silicon solar cells, which will promote their use, they still have drawbacks despite their affordability and simplicity of manufacture. DSSCs' primary drawbacks can be summed up as low stability, low efficiency, and low scalability. Voc (open circuit voltage), Isc (short circuit current), internal resistances, and FF (fill factor) are just a few of the variables that affect efficiency. To generate excited electrons and energy that is subsequently transferred to a material, such as titanium dioxide (TiO_2), DSSCs employ an organic dye to absorb incident light rays. The energy is therefore collected through a transparent conducting medium. The energy is therefore collected through a transparent conducting medium. Because these cells contain a variety of fundamental components and their numerous possible combinations, this task poses experimental challenges. Despite significant experimental efforts to improve them, the obtained photo-conversion efficiencies remain low to this day. Its conversion efficiency currently falls short of the norm for the majority of solar technology, ranging from 8% to 11%. By lowering some internal resistances, the conversion efficiency could be increased. Reducing the gaps between electrodes, modifying the roughness factor, and varying the thickness of the electrode conducting layer are some methods for lowering the internal resistances of the cell. According to stability studies, DSSCs are not yet dependable for long-term performance and efficiency predictions. More research is required on the DSSC system's sealing process and material [Adedokun, O., Titilope, K., & Awodugba, A. O. (2016)].

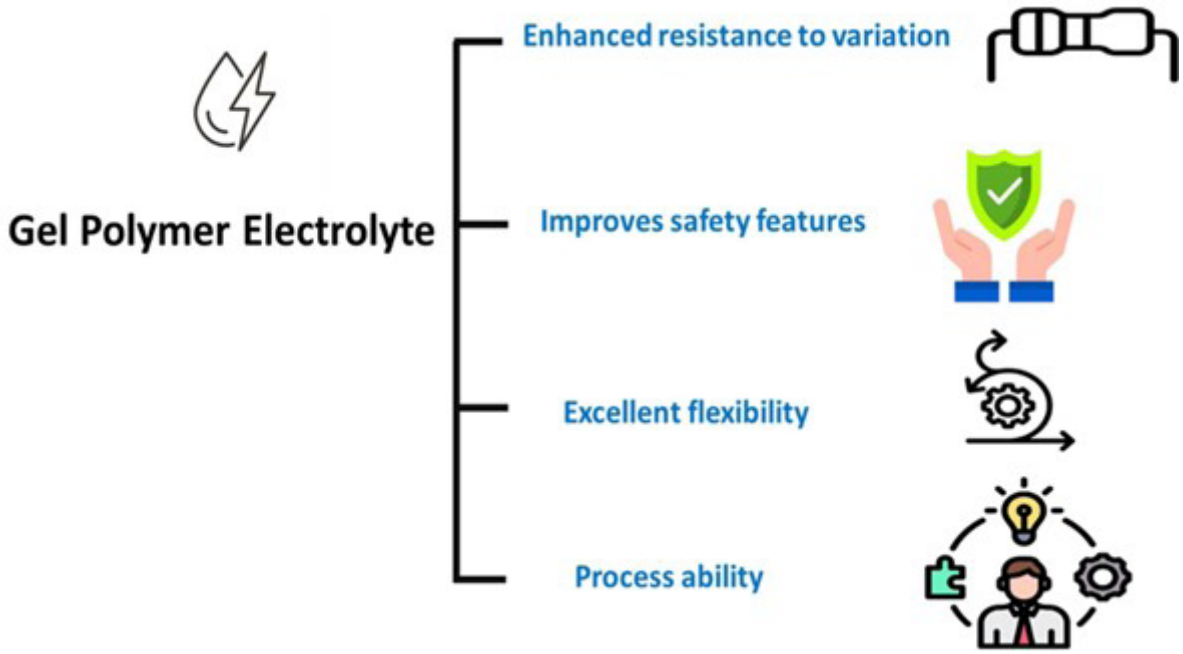
Because of their low cost and extremely high theoretical energy density, lithium-sulfur (Li–S) batteries are anticipated to be the next generation of energy storage technology. However, the two main obstacles to commercially viable Li–S batteries are the uncontrollable growth of lithium dendrites and the infamous shuttle effect of higher-order polysulfides. Here, the bi-functional gel polymer electrolyte (GPE) is polymerised in situ to address these two primary issues. Dyesensitised solar cells (DSSC) are a subset of photoelectrochemical (PEC) solar cells because of their shared reliance on an electrolyte. Based on reports of up to 11% efficiency in the literature, they represent a potentially significant advancement in solar technology [Quan et al., 2024]. Later on, though, a prototype with a 15% solar cell efficiency was revealed [Subramanian, A., Murugapoopathi, S., & Amesho, K. T. T. (2024)]. A DSSC normally consists of the following components: dye sensitizer, titanium dioxide photo anode, $I3^-/I^-$ redox electrolyte, and counter electrode [[Patni, N., & Pillai, S. G. (2025)]].

Generally speaking, liquid electrolytes offer several noteworthy advantages, such as low viscosity, high conductivity, high conversion efficiency, and simplicity of preparation. The liquid electrolyte's primary problems are that it tends to flow, dries up in a few weeks, becomes unstable over time, and may desorb and photodegrade the dyes that are attached to it. The quasi-solid electrolyte can be used to counteract other problems, such as temperature changes caused by exposure to sunlight or high voltage [Zakariya et al., 2024]. Despite having already attained high conversion efficiencies, liquid electrolyte-based DSSCs have also created significant challenges for their practical application. For instance, because of their high volatility, DSSCs' performance declines over extended periods of operation due to solvent losses [O'Regan et al., 2002]. Several work have been done to replace liquid electrolytes with solid or quasi-solid type charge transport materials to get around these issues [O'Regan, et al (2002)]. High ionic conductivities, which are attained by "trapping" a liquid electrolyte in polymer cages created in a host matrix, as well as good contacting and filling properties of the nanostructured electrode and counter electrode, are some of the benefits of gel polymer electrolytes when compared to other types of charge transport materials. Consequently, there has been a lot of interest in gel polymer electrolytes. Quasi-solid state dye-sensitized solar cells have already employed several gel electrolyte types based on various polymer types [Wang et al., 2003].

A liquid electrolyte is encased in polymer cages to create the GPEs. GPEs have several advantages over conventional polymer electrolytes, including low vapour pressure, superior wetting and filling characteristics between the nanostructured electrode and counter-electrode, higher ionic conductivity, and exceptional thermal stability. These features contribute to the DSSCs' exceptional long-term stability, as seen by their diverse

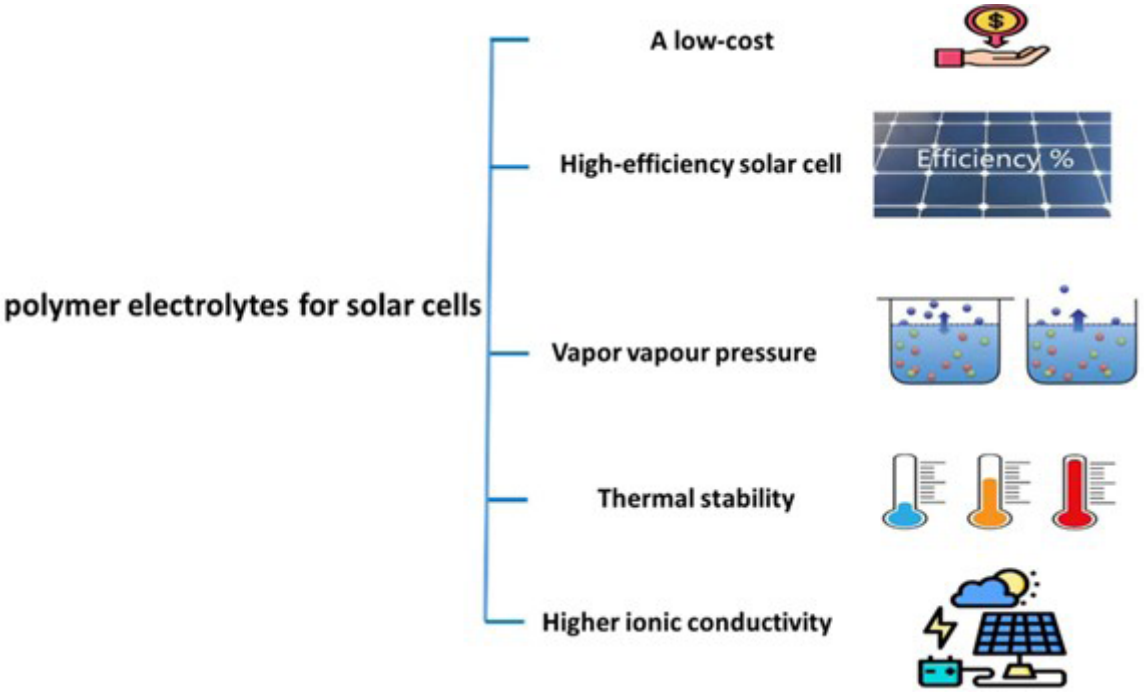
range of applications. **Figure 20** shows the Gel polymer electrolytes' (GPEs') benefits. Improving these GPEs' ionic conductivities is essential for achieving high DSSC conversion efficiency. Traditional (solid) polymer electrolytes have comparatively poor ambient ionic conductivity because of the high crystallinity of the polymers. The synthesis and characterisation of GPEs with enhanced ionic conductivity at room temperature have been the main topics of recent studies in this area. Room temperature ionic liquids, or RTILs, are both plasticisers and ion sources. To increase ionic conductivity to a feasible level (at least 1 mS/cm), highly conductive polymer gels composed of a polymer matrix, plasticiser, and redox couple salts have been thoroughly investigated. Wang et al. [2003] produced a series of quasisolid-state DSSCs by combining methoxypropionitrile (MPN)-based gel electrolytes with 5 weight percent poly (vinylidenefluoride-co-hexafluoropropylene) (PVDF-HFP). These polymer gels' conductivities were close to 10 mS/cm at 1 Sun illumination, and their cell efficiencies exceeded 6%. A PVDF-based polymer gel system with a cross-linking reinforced network of polyethylene glycol dimethacrylate (PEGDMA) was developed by Cheng et al. [2004]. It possessed good mechanical toughness and ionic conductivity.

Figure 20. Advantages of gel polymer electrolytes (GPEs).



GPEs have several advantages over conventional polymer electrolytes, including low vapour pressure, superior wetting and filling characteristics between the nanostructured electrode and counter-electrode, higher ionic conductivity, and exceptional thermal stability. In **Figure 21**, the Polymer electrolyte benefits for solar cells. Numerous new opportunities have been made possible by the remarkable and recent developments in the characterisation and synthesis of nanocrystalline materials. Contrary to expectations, devices based on interpenetrating networks of mesoscopic semiconductors have demonstrated remarkably high conversion efficiencies that are comparable to those of conventional devices [Nujud et al, 2023]. The prototype of this class of devices, dyesensitised solar cells, combines a sensitiser, a light-absorbing substance, with a wide bandgap semiconductor with a nanocrystalline morphology to produce optical absorption and charge separation [O'Regan, B., Grätzel, M. 1991][Nujud et al 2023].

Figure 21. Advantages of polymer electrolytes for solar cells



CONCLUSION

Because polymer-based electrolytes are inexpensive, flexible, long-lasting, safe, mechanically robust, and have high ionic conductivity, they lessen pollution and energy consumption problems. Nowadays, polymer electrolyte is a novel material because it is utilised as the electrolyte in solar cells, which are energy storage devices. Crystalline and semicrystalline components make up polymers. There are several ways to change the properties of polymers. To improve DSSC performance for sustainability in solar energy applications, the current study focuses on improving interface stability and exploring novel electrolyte compositions. Notwithstanding advancements, challenges still exist in articulating fundamental ideas and research methodologies in DSSC technology. Widespread research has been conducted on the substantial potential of DSSCs in photovoltaic production. Numerous studies are underway to improve efficiency by changing or modifying key cell components, such as electrolytes.

REFERENCES

1. Ngidi, N. P. D., Ollengo, M. A., & Nyamori, V. O. (2019). Heteroatom-doped graphene and its application as a counter electrode in dye-sensitized solar cells. International Journal of Energy Research, 43(5), 1702–1734. https://doi.org/10.1002/ER.4326.

2. Kalaivani, G., Sumathi, T., Nath, S. S., Manikandababu, C. S., Al-Taisan, N. A., Souayeh, B., Zaidi, N., & Alam, M. W. (2025). Enhancement of photovoltaic performance of graphene-TiO2 photoanode for dye-sensitized solar cells (DSSCs). Journal of Materials Science: Materials in Electronics 2025 36:2, 36(2), 1–12. https://doi.org/10.1007/S10854-024-14153-4.

3. Orona-Navar, A., Aguilar-Hernández, I., Cerdán-Pasarán, A., López-Luke, T., Rodríguez-Delgado, M., Cárdenas-Chávez, D. L., Cepeda-Pérez, E., & Ornelas-Soto, N. (2017). Astaxanthin from Haematococcus pluvialis as a natural photosensitizer for dye-sensitized solar cells. Algal Research, 26, 15–24. https://doi.org/10.1016/J.ALGAL.2017.06.027.

4. Nujud Badawi, M. Bhuyan, Mohammad Luqman, Rayed S. Alshareef, Mohammad Raf Hatshan, Abdulrahman Al-Warthan, Syed Farooq Adil .(2024). MXenes the future of solid-state supercapacitors: Status, challenges, prospects, and applications. Arabian Journal of Chemistry. https://doi.org/10.1016/j.arabjc.2024.105866.

5. Khan, M. J., Ahirwar, A., Sirotiya, V., Rai, A., Varjani De, S., & Vinayak, V. (2023). Nanoengineering TiO 2 for evaluating performance in dye sensitized solar cells with natural dyes. Pubs.Rsc.OrgMJ Khan, A Ahirwar, V Sirotiya, A Rai, S Varjani, V VinayakRSC Advances, 2023•pubs.Rsc.Org, 13(32), 22630–22638. https://doi.org/10.1039/d3ra02927a.

6. Tropea, A., Spadaro, D., Citro, I., Lanza, M., Trocino, S., Tella, R. la, Giuffrida, D., Mussagy, C. U., Mondello, L., & Calogero, G. (2025). The influence of microbial sources

on astaxanthin implementation as sensitizer in dye sensitized solar cells (DSSCs). Journal of Photochemistry and Photobiology A: Chemistry, 461, 116174. https://doi.org/10.1016/J.JPHOTOCHEM.2024.116174.

7. Tropea, A., Spadaro, D., Trocino, S., Giuffrida, D., Salerno, T. M. G., Ruiz-Sanchez, J. P., Montañez, J., Morales-Oyervides, L., Dufossé, L., Mondello, L., & Calogero, G. (2024). Development of dye-sensitized solar cells using pigment extracts produced by Talaromyces atroroseus GH2. Photochemical and Photobiological Sciences, 23(5), 941–955. https://doi.org/10.1007/S43630-024-00566-X/FIGURES/8.

8. Bai, Q., Cheng, Y., Wang, W., Chen, J., & Sun, H. (2024). Polythiophene and its derivatives for all-polymer solar cells. Journal of Materials Chemistry A, 12(27), 16251–16267. https://doi.org/10.1039/D4TA02245A.

9. Fonteyn, P., Lizin, S., Cells, W. M.-S. E. M. and S., & 2020, undefined. (n.d.). The evolution of the most important research topics in organic and perovskite solar cell research from 2008 to 2017: A bibliometric literature review using bibliographic . ElsevierP Fonteyn, S Lizin, W MaesSolar Energy Materials and Solar Cells, 2020•Elsevier. Retrieved January 9, 2025, from https://www.sciencedirect.com/science/article/pii/S0927024819306531.

10. Arefinia, Z., & Samajdar, D. P. (2021). Novel semi-analytical optoelectronic modeling based on homogenization theory for realistic plasmonic polymer solar cells. Scientific Reports 2021 11:1, 11(1), 1–18. https://doi.org/10.1038/s41598-021-82525-5.

11. Li, Z., Xu, X., Zhang, W., Meng, X., Ma, W., Yartsev, A., Inganäs, O., Andersson, M. R., Janssen, R. A. J., & Wang, E. (2016). High Performance All-Polymer Solar Cells by Synergistic Effects of Fine-Tuned Crystallinity and Solvent Annealing. Journal of the American Chemical Society, 138(34), 10935–10944. https://doi.org/10.1021/JACS.6B04822/SUPPL_FILE/JA6B04822_SI_001.PDF.

12. Yu, H., Wang, Y., Kwok, C. H., Zhou, R., Yao, Z., Mukherjee, S., Sergeev, A., Hu, H., Fu, Y., Ng, H. M., Chen, L., Zhang, D., Zhao, D., Zheng, Z., Lu, X., Yin, H., Wong, K. S., Ade, H., Zhang, C., … Yan, H. (2024). A polymer acceptor with double-decker configuration enhances molecular packing for high-performance all-polymer solar cells. Joule, 8(8), 2304–2324. https://doi.org/10.1016/j.joule.2024.06.010.

13. Cheng, P., & Zhan, X. (2016). Stability of organic solar cells: challenges and strategies. Chemical Society Reviews, 45(9), 2544–2582. https://doi.org/10.1039/C5CS00593K.

14. Guo, W., Xu, Z., Zhang, F., Xie, S., Xu, H., & Liu, X. Y. (2016). Recent Development of Transparent Conducting Oxide-Free Flexible Thin-Film Solar Cells. Advanced Functional Materials, 26(48), 8855–8884. https://doi.org/10.1002/ADFM.201603378.

15. Duan, L., Science, A. U.-A., & 2020, undefined. (2020). Progress in stability of organic solar cells. Wiley Online LibraryL Duan, A UddinAdvanced Science, 2020•Wiley Online Library, 7(11). https://doi.org/10.1002/advs.201903259.

16. Liu, Q., Jiang, Y., Jin, K., Qin, J., Xu, J., Li, W., Xiong, J., Liu, J., Xiao, Z., Sun, K., Yang, S., Zhang, X., & Ding, L. (2020). 18% Efficiency organic solar cells. Science Bulletin, 65(4), 272–275. https://doi.org/10.1016/J.SCIB.2020.01.001.

17. Tian, X., Zhang, Y., Hao, Y., Cui, Y., Wang, W., Shi, F., Wang, H., Wei, B., & Huang, W. (2015). Semitransparent inverted organic solar cell with improved absorption and reasonable transparency perception based on the nanopatterned MoO 3 / Ag / MoO 3 anode. Journal of Nanophotonics, 9(1), 093043. https://doi.org/10.1117/1.JNP.9.093043.

18. Joseph, B., … T. P.-I. J. of, & 2019, undefined. (2019). Semitransparent building-integrated photovoltaic: review on energy performance, challenges, and future potential. Wiley Online LibraryB Joseph, T Pogrebnaya, B KichongeInternational Journal of Photoenergy, 2019•Wiley Online Library, 2019. https://doi.org/10.1155/2019/5214150.

19. Khan, M. J., Ahirwar, A., Sirotiya, V., Rai, A., Varjani De, S., & Vinayak, V. (2023). Nanoengineering TiO 2 for evaluating performance in dye sensitized solar cells with natural dyes. Pubs.Rsc.OrgMJ Khan, A Ahirwar, V Sirotiya, A Rai, S Varjani, V VinayakRSC Advances, 2023•pubs.Rsc.Org, 13(32), 22630–22638. https://doi.org/10.1039/d3ra02927a.

20. Corcoles, L., Abad, J., Padilla, J., Solar, A. U.-S. E. M. and, & 2015, undefined. (n.d.). Wavelength influence on the photodegradation of P3HT: PCBM organic solar cells. ElsevierL Corcoles, J Abad, J Padilla, A UrbinaSolar Energy Materials and Solar Cells, 2015•Elsevier. https://www.sciencedirect.com/science/article/pii/S0927024815002925.

21. Jan Anton, L., Bartesaghi, D., Ye, G., Chiechi, R. C., Jan Anton Koster, L., Bartesaghi, D., A Koster, L. J., Ye, G., & Chiechi, R. C. (2016). Compatibility of PTB7 and PCBM Solar Cells. Wiley Online LibraryD Bartesaghi, G Ye, RC Chiechi, LJA KosterAdvanced Energy Materials, 2016•Wiley Online Library, 6(13). https://doi.org/10.1002/aenm.201502338.

22. Li, Y., Xu, G., Cui, C., & Li, Y. (2018). Flexible and Semitransparent Organic Solar Cells. Advanced Energy Materials, 8(7), 1701791. https://doi.org/10.1002/AENM.201701791.

23. Yuan, X., Zhao, Y., Xie, D., Pan, L., Liu, X., Duan, C., Huang, F., & Cao, Y. (2022). Polythiophenes for organic solar cells with efficiency surpassing 17%. Joule, 6(3), 647–661. https://doi.org/10.1016/J.JOULE.2022.02.006/ATTACHMENT/7515D4F0-59F4-4C57-B69AD4387FF402D3/MMC2.PDF.

24. Wang, Q., Li, M., Zhang, X., Qin, Y., Wang, J., ... J. Z.-, & 2019, undefined. (2019). Carboxylatesubstituted polythiophenes for efficient fullerene-free polymer solar cells: the effect of chlorination on their properties. ACS PublicationsQ Wang, M Li, X Zhang, Y Qin, J Wang, J Zhang, J Hou, RAJ Janssen, Y GengMacromolecules, 2019•ACS Publications, 52(12), 4464–4474. https://doi.org/10.1021/acs.macromol.9b00793.

25. Yang, C., Zhang, S., Ren, J., Gao, M., Bi, P., ... L. Y.-E. & E., & 2020, undefined. (n.d.). Molecular design of a non-fullerene acceptor enables a P3HT-based organic solar cell with 9.46% efficiency. Pubs.Rsc.OrgC Yang, S Zhang, J Ren, M Gao, P Bi, L Ye, J HouEnergy & Environmental Science,2020•https://pubs.rsc.org/en/content/articlehtml/2020/ee/d0ee01763a.

26. Yang, C., Zhang, S., Ren, J., Gao, M., Bi, P., Ye, L., Hou, J., Zhang, S., Ye, L., & Hou, J. (2020). Molecular design of a non-fullerene acceptor enables a P3HT-based organic solar cell with 9.46% efficiency. Energy & Environmental Science, 13(9), 2864–2869. https://doi.org/10.1039/D0EE01763A.

27. Liang, Z., Li, M., Wang, Q., Qin, Y., Stuard, S., Joule, Z. P.-, & 2020, undefined. (2020). Optimization requirements of efficient polythiophene: nonfullerene organic solar cells. Cell.ComZ Liang, M Li, Q Wang, Y Qin, SJ Stuard, Z Peng, Y Deng, H Ade, L Ye, Y GengJoule, 2020•cell.Com, 4, 1278–1295. https://doi.org/10.1016/j.joule.2020.04.014.

28. Su, Z., Liu, W., Song, H., Wei, N., Chen, J., Lin, Y., Zhang, W., Xu, X., Ma, Z., Li, C., Zhang, A., Liu, Y., & Bo, Z. (2024). Efficient Synthesis of High-Performance Wide-Bandgap Polymers Based on Difluoronaphthodithiophene: Fluorination Position Impact on Photovoltaic Performance. ACS Applied Polymer Materials. https://doi.org/10.1021/ACSAPM.4C02206.

29. Jia, X., Chen, Z., Duan, C., Wang, Z., Yin, Q., Huang, F., & Cao, Y. (2019). Polythiophene derivatives compatible with both fullerene and non-fullerene acceptors for polymer solar cells. Journal of Materials Chemistry C, 7(2), 314–323. https://doi.org/10.1039/C8TC04746D.

30. Cai, P., Song, C., Du, Y., Wang, J., Wang, J., Sun, L., Gao, F., & Xue, Q. (2025). Recent Progress of Solution-Processed Thickness-Insensitive Cathode Interlayers for High-Performance Organic Solar Cells. Advanced Functional Materials, 2422023. https://doi.org/10.1002/ADFM.202422023.

31. Yao, J., Diao, Y., Zhu, Y., Xu, X., Fu, R., Gao, B., Xiang, H., Wang, X., & Li, Y. (2024). PEDOT quality: another key factor determining the thermal stability of organic solar cells. Journal of Materials Chemistry C. https://doi.org/10.1039/D4TC03528C.

32. Liu, L., Yu, F., Hu, D., Jiang, X., Huang, P., Li, Y., Tian, G., Lei, H., Wu, S., Tu, K., Chen, C., Gu, T., Chen, Y., Duan, T., & Xiao, Z. (2024). Breaking the symmetry of interfacial molecules with push–pull substituents enables 19.67% efficiency organic solar cells featuring enhanced charge extraction. Energy & Environmental Science. https://doi.org/10.1039/D4EE04515G.

33. Chen, Z., El, M., Boudia, A., & Zhao, C. (2025). Highly Stable Inverted Organic Solar Cell Structure Using Three Efficient Electron Transport Layers. Energies 2025, Vol. 18, Page 167, 18(1), 167. https://doi.org/10.3390/EN18010167.

34. Zhu, L., Zhang, M., Xu, J., Li, C., Yan, J., Zhou, G., Zhong, W., Hao, T., Song, J., Xue, X., Zhou, Z., Zeng, R., Zhu, H., Chen, C. C., MacKenzie, R. C. I., Zou, Y., Nelson, J., Zhang, Y., Sun, Y., & Liu, F. (2022). Single-junction organic solar cells with over 19% efficiency enabled by a refined double-fibril network morphology. Nature Materials 2022 21:6, 21(6), 656–663. https://doi.org/10.1038/s41563-022-01244-y.

35. Li, Y., Wang, B., Chen, L., Yuan, Y., Fu, J., Geng, C., Wan, J., & Wang, H. Q. (2024). Optimisation of active layers for efficient binary organic solar cells. Physical

Chemistry Chemical Physics, 27(1), 301–307. https://doi.org/10.1039/D4CP03492A.

36. Benaya, N., Taouti, M. M., Bougnina, K., Deghfel, B., & Zoukel, A. (2025). Gold nanoparticles in P3HT: PCBM active layer: A simulation of new organic solar cell designs. Solid-State Electronics, 109056. https://doi.org/10.1016/J.SSE.2025.109056.

37. Lobregas, M. O. S., & Camacho, D. H. (2019). Gel polymer electrolyte system based on starch grafted with ionic liquid: Synthesis, characterization and its application in dye-sensitized solar cell. Electrochimica Acta, 298, 219–228. https://doi.org/10.1016/J.ELECTACTA.2018.12.090.

38. Primiceri, V., Pugliese, M., Prontera, C. T., Monteduro, A. G., Esposito, M., Maggiore, A., Cannavale, A., Giannuzzi, R., Gigli, G., & Maiorano, V. (2022). Low-cost gel polymeric electrolytes for electrochromic applications. Solar Energy Materials and Solar Cells, 240, 111657. https://doi.org/10.1016/J.SOLMAT.2022.111657.

39. Theodosiou, Dokouzis, A., Antoniou, I., & Leftheriotis, G. (2019). Gel electrolytes for partly covered photoelectrochromic devices. Solar Energy Materials and Solar Cells, 202, 110124. https://doi.org/10.1016/J.SOLMAT.2019.110124.

40. Watanabe, Y., Nagashima, T., Nakamura, K., & Kobayashi, N. (2012). Continuous-tone images obtained using three primary-color electrochromic cells containing gel electrolyte. Solar Energy Materials and Solar Cells, 104, 140–145. https://doi.org/10.1016/J.SOLMAT.2012.05.019.

41. Périé, C., Mary, V., Faceira, B., & Rougier, A. (2022). Colored electrolytes for electrochromic devices. Solar Energy Materials and Solar Cells, 238, 111626. https://doi.org/10.1016/J.SOLMAT.2022.111626.

42. Zhou, J., Wang, J., Li, H., & Shen, F. (2018). A hybrid gel polymer electrolyte with good stability and its application in electrochromic device. Journal of Materials Science: Materials in Electronics, 29(7), 6068–6076. https://doi.org/10.1007/S10854-018-8581-7/METRICS.

43. Utracki, L. (n.d.). Commercial polymer blends. 2013. Retrieved January 10, 2025, from https://books.google.com/books?hl=ar&lr=&id=bYvkBwAAQBAJ&oi=fnd&pg=PR13&ots=vz6GX3oPE5&sig=4x5n5m92R_J1ka-3CHIiISBVkyTg.

44. Mantia, F. la, Morreale, M., Botta, L., ... M. M.-P. D., & 2017, undefined. (n.d.). Degradation of polymer blends: A brief review. ElsevierFP La Mantia, M Morreale, L Botta, MC Mistretta, M Ceraulo, R Scaffaro Polymer Degradation and Stability, 2017•Elsevier. https://www.sciencedirect.com/science/article/pii/S014139101730201X.

45. Utracki, L., & Wilkie, C. (n.d.). Polymer blends handbook. 2002.https://www.researchgate.net/profile/Doufnoune-Rachida/post/What_are_some_examples_of_novel_models_predicting_viscosity_of_immiscible_polymer_blends/attachment/5fe986293b21a2000164e324/AS%3A973616841768961%4016091397523 89/download/11148_15a.pdf%20R%20%20%20%20%20%20%C2%A3%C3%98%E2%80%A2%20%C2%A3%C3%98%E2%80%A2%20%20%20%20%20%20%20%20%20.

46. Aframehr, W. M., Molki, B., Bagheri, R., Heidarian, P., & Davodi, S. M. (2020). Characterisation and enhancement of the gas separation properties of mixed matrix membranes: Polyimide with nickel oxide nanoparticles. Chemical Engineering Research and Design, 153, 789–805. https://doi.org/10.1016/J.CHERD.2019.11.006.

47. Chen, Z. A., Zhao, B., Xin, J., & Liu, Y. (2024). A new segment-level mixing strategy to improve the gas separation performances of carbon molecular sieve membrane derived from polymer blends. Journal of Membrane Science, 695, 122481. https://doi.org/10.1016/J.MEMSCI.2024.122481.

48. Li, X., Ke, H., Li, S., Gao, M., Li, S., Yu, J., Xie, H., Zhou, K., Zhang, K., & Ye, L. (2024). Intrinsically Stretchable Organic Photovoltaic Cells with Improved Mechanical Durability and Stability via Dual-Donor Polymer Blending. Advanced Functional Materials, 34(29), 2400702. https://doi.org/10.1002/ADFM.202400702.

49. Ma, R., Li, H., dela Peña, T. A., Xie, X., Fong, P. W. K., Wei, Q., Yan, C., Wu, J., Cheng, P., Li, M., & Li, G. (2024). Tunable Donor Aggregation Dominance in a Ternary Matrix of All-Polymer Blends with Improved Efficiency and Stability. Advanced Materials, 36(15), 2304632. https://doi.org/10.1002/ADMA.202304632.

50. Kuang, T., Guo, H., Guo, W., Liu, W., Li, W., Saeb, M. R., Vatankhah-Varnosfaderani, M., & Sheiko, S. S. (2024). Boosting the Strength and Toughness of Polymer Blends via Ligand-Modulated MOFs. Advanced Science, 11(45), 2407593. https://doi.org/10.1002/ADVS.202407593.

51. Gorjian, S., Calise, F., Kant, K., ... M. A.-J. of C., & 2021. opportunities for implementation of solar energy technologies in agricultural greenhouses .ElsevierS Gorjian, F Calise, K Kant, MS Ahamed, B Copertaro, G Najafi, X Zhang, M AghaeiJournal of Cleaner Production, 2021• https://www.sciencedirect.com/science/article/pii/S095965262034851.

52. E. Bellini. (2020) Global solar capacity may reach 1,448 GW in 2024, PV Mag. https://www.pvmagazine.com/2020/06/16/global-solar-capacity-may-reach-1448-gw-in-2024.

53. Dai, Y., Energies, Y. B.-, & 2020, undefined. (2020). Performance improvement for building integrated photovoltaics in practice: A review. Mdpi.ComY Dai, Y BaiEnergies, 2020•mdpi.Com. https://doi.org/10.3390/en14010178.

54. Duman, A., Energy, Ö. G.-R., & 2020, undefined. (n.d.). Economic analysis of grid-connected residential rooftop PV systems in Turkey. ElsevierAC Duman, Ö GülerRenewable Energy, 2020•Elsevier. https://www.sciencedirect.com/science/article/pii/S0960148119316544.

55. Kuang, Y., Zhang, Y., Zhou, B., Li, C., Cao, Y., Li, L., & Zeng, L. (2016). A review of renewable energy utilization in islands. Renewable and Sustainable Energy Reviews, 59, 504–513. https://doi.org/10.1016/J.RSER.2016.01.014.

56. Barbosa, M. dos S. (2022). Ciências exatas e da terra: Conhecimentos didático-pedagógicos e o ensino-aprendizagem. Ciências Exatas e Da Terra: Conhecimentos Didático-Pedagógicos e o Ensino-Aprendizagem. https://doi.org/10.22533/AT.ED.224220408.

57. Nature, S. F.-, & 2004, undefined. (n.d.). The path to ubiquitous and low-cost organic electronic appliances on plastic. Nature.ComSR Forrestnature, 2004•nature.Com. Retrieved January 10, 2025, from https://www.nature.com/articles/nature02498.

58. Sampaio, P. G. V., & González, M. O. A. (2022). A review on organic photovoltaic cell. International Journal of Energy Research, 46(13), 17813–17828. https://doi.org/10.1002/ER.8456.

59. Vishnu Subramaniam, S., van der Wiel, B., Sauermann, T., Kutsarov, D., Schilinsky, P., Pätzold, R., Baumann, R. R., & Meier, S. B. (2020). Late-Stage Customization in Volume Production of Organic Photovoltaics. ACS Applied Electronic Materials, 2(3), 756–762. https://doi.org/10.1021/ACSAELM.9B00826/ASSET/IMAGES/MEDIUM/EL9B00826_0008.GIF.

60. Meng, L., Zhang, Y., Wan, X., Li, C., Zhang, X., Wang, Y., Ke, X., Xiao, Z., Ding, L., Xia, R., Yip, H. L., Cao, Y., & Chen, Y. (2018). Organic and solution-processed tandem solar cells with 17.3% efficiency. Science, 361(6407), 1094–1098. https://doi.org/10.1126/SCIENCE.AAT2612.

61. Li, G., Zhu, R., & Yang, Y. (2012). Polymer solar cells. Nature Photonics 2012 6:3, 6(3), 153–161. https://doi.org/10.1038/nphoton.2012.11.

62. Tsang, M., Sonnemann, G., and, D. B.-S. E. M., & 2016, undefined. (n.d.). Life-cycle assessment of cradle-to-grave opportunities and environmental impacts of organic photovoltaic solar panels compared to conventional technologies. ElsevierMP Tsang, GW Sonnemann, DM BassaniSolar Energy Materials and Solar Cells, 2016•Elsevier. Retrieved January 10, 2025. https://www.sciencedirect.com/science/article/pii/S0927024816300381.

63. Yue, D., Khatav, P., You, F., & Darling, S. B. (2012). Deciphering the uncertainties in life cycle energy and environmental analysis of organic photovoltaics. Energy & Environmental Science, 5(11), 9163–9172. https://doi.org/10.1039/C2EE22597B.

64. Lizin, S., van Passel, S., de Schepper, E., Maes, W., Lutsen, L., Manca, J., & Vanderzande, D. (2013). Life cycle analyses of organic photovoltaics: a review. Energy & Environmental Science, 6(11), 3136–3149. https://doi.org/10.1039/C3EE42653J.

65. Agger, A. (2016). Third Generation Storytelling video om bogen. Workz. https://books.google.com/books/about/Third_Generation_Photovoltaics.html?hl=ar&id=UCaDwAAQBAJ.

66. Tsang, M., Sonnemann, G., and, D. B.-S. E. M., & 2016, undefined. (n.d.). Life-cycle assessment of cradle-to-grave opportunities and environmental impacts of organic photovoltaic solar panels compared to conventional technologies. Elsevier. Retrieved January 10, 2025, from https://www.sciencedirect.com/science/article/pii/S0927024816300381.

67. Lizin, S., Passel, S. van, de Schepper, E., Maes, W., Lutsen, L., Manca, J., & Vanderzande, D. (n.d.). Life cycle analyses of organic photovoltaics: a review. Pubs.Rsc.

OrgS Lizin, S Van Passel, E De Schepper, W Maes, L Lutsen, J Manca, D VanderzandeEnergy & Environmental Science, 2013•pubs.Rsc.Org. https://doi.org/10.1039/c3ee42653j.

68. Espinosa, N., Laurent, A., Science, F. K.-E. & E., & 2015, undefined. (n.d.). Ecodesign of organic photovoltaic modules from Danish and Chinese perspectives. Pubs.Rsc.OrgN Espinosa, A Laurent, FC KrebsEnergy & Environmental Science, 2015•pubs.Rsc.Org. Retrieved January 10, 2025, from https://pubs.rsc.org/en/content/articlehtml/2015/ee/c5ee01763g.

69. Tsang, M. P., Sonnemann, G. W., & Bassani, D. M. (2016). Life-cycle assessment of cradle-tograve opportunities and environmental impacts of organic photovoltaic solar panels compared to conventional technologies. Solar Energy Materials and Solar Cells, 156, 37–48. https://doi.org/10.1016/J.SOLMAT.2016.04.024.

70. Sherwani, A., Reviews, J. U.-R. and S. E., & 2010, undefined. (n.d.). Life cycle assessment of solar PV based electricity generation systems: A review. ElsevierAF Sherwani, JA UsmaniRenewable and Sustainable Energy Reviews, 2010•Elsevier. Retrieved January 10, 2025, from https://www.sciencedirect.com/science/article/pii/S1364032109001907.

71. Müller, A., Friedrich, L., Reichel, C., … S. H.-S. E. M., & 2021, undefined. (n.d.). A comparative life cycle assessment of silicon PV modules: Impact of module design, manufacturing location and inventory. ElsevierA Müller, L Friedrich, C Reichel, S Herceg, M Mittag, DH NeuhausSolar Energy Materials and Solar Cells, 2021•Elsevier. Retrieved January 10, 2025, from https://www.sciencedirect.com/science/article/pii/S0927024821003202.

72. Krebs-Moberg, M., Pitz, M., Dorsette, T., Energy, S. G.-R., & 2021, undefined. (n.d.). Third generation of photovoltaic panels: A life cycle assessment. ElsevierM Krebs-Moberg, M Pitz, TL Dorsette, SH GheewalaRenewable Energy, 2021•Elsevier. Retrieved January 10, 2025, from https://www.sciencedirect.com/science/article/pii/S0960148120314798.

73. Krebs-Moberg, M., Pitz, M., Dorsette, T. L., & Gheewala, S. H. (2021). Third generation of photovoltaic panels: A life cycle assessment. Renewable Energy, 164, 556–565. https://doi.org/10.1016/J.RENENE.2020.09.054.

74. Li, Q., Monticelli, C., & Zanelli, A. (2022). Life cycle assessment of organic solar cells and perovskite solar cells with graphene transparent electrodes. Renewable Energy, 195, 906–917. https://doi.org/10.1016/J.RENENE.2022.06.075.

75. Gong, J., Darling, S., Science, F. Y.-E. & E., & 2015, undefined. (2015). Perovskite photovoltaics: life-cycle assessment of energy and environmental impacts. Pubs.Rsc.OrgJ Gong, SB Darling, F You Energy & Environmental Science, 2015•pubs.Rsc.Org. https://pubs.rsc.org/en/content/articlehtml/2015/ee/c5ee00615e.

76. A dos Reis Benatto, G., Espinosa, N., & Krebs, F. C. (2017). Life-Cycle Assessment of Solar Charger with Integrated Organic Photovoltaics. Advanced Engineering Materials, 19(8). https://doi.org/10.1002/ADEM.201700124.

77. Espinosa, N., Laurent, A., Science, F. K.-E. & E., & 2015, undefined. (n.d.). Ecodesign of organic photovoltaic modules from Danish and Chinese perspectives. Pubs.Rsc.OrgN Espinosa, A Laurent, FC KrebsEnergy & Environmental Science, 2015•pubs.Rsc.Org. Retrieved January 10, 2025, from https://pubs.rsc.org/en/content/articlehtml/2015/ee/c5ee01763g.

78. Espinosa, N., Hösel, M., … M. J.-E. & E., & 2014, undefined. (2014). Large scale deployment of polymer solar cells on land, on sea and in the air. Pubs.Rsc.OrgN Espinosa, M Hösel, M Jørgensen, FC KrebsEnergy & Environmental Science, 2014•pubs.Rsc.Org. https://doi.org/10.1039/c3ee43212b.

79. Roes, A. L., Alsema, E. A., Blok, K., & Patel, M. K. (2009). Ex-ante environmental and economic evaluation of polymer photovoltaics. Progress in Photovoltaics: Research and Applications, 17(6), 372–393. https://doi.org/10.1002/PIP.891.

80. Anctil, A., Babbitt, C. W., Raffaelle, R. P., & Landi, B. J. (2013). Cumulative energy demand for small molecule and polymer photovoltaics. Progress in Photovoltaics: Research and Applications, 21(7), 1541–1554. https://doi.org/10.1002/PIP.2226.

81. Chatzisideris, M., Laurent, A., Hauschild, M., Annals, F. K.-C., & 2017, undefined. (2025). Environmental impacts of electricity self-consumption from organic photovoltaic battery systems at industrial facilities in Denmark. Elsevier, 66, 45–48. https://doi.org/10.1016/j.cirp.2017.04.100.

82. Chatzisideris, M. D. ;, Ohms, P. K. ;, Espinosa, N. ;, Krebs,

F. C. ;, & Laurent, A. (n.d.). Economic and environmental performances of organic photovoltaics with battery storage for residential selfconsumption. ElsevierMD Chatzisideris, PK Ohms, N Espinosa, FC Krebs, A LaurentApplied Energy, 2019•Elsevier. https://doi.org/10.1016/j.apenergy.2019.113977.

83. Lizin, S., Passel, S. van, de Schepper, E., Maes, W., Lutsen, L., Manca, J., & Vanderzande, D. (n.d.). Life cycle analyses of organic photovoltaics: a review. Pubs.Rsc.OrgS Lizin, S Van Passel, E De Schepper, W Maes, L Lutsen, J Manca, D VanderzandeEnergy & Environmental Science, 2013•pubs.Rsc.Org. https://doi.org/10.1039/c3ee42653j.

84. Glogic, E., Weyand, S., Tsang, M., … S. Y.-J. of cleaner, & 2019, undefined. (n.d.). Life cycle assessment of organic photovoltaic charger use in Europe: The role of product use intensity and irradiation. ElsevierE Glogic, S Weyand, MP Tsang, SB Young, L Schebek, G SonnemannJournal of Cleaner Production, 2019•Elsevier. Retrieved January 10, 2025, from https://www.sciencedirect.com/science/article/pii/S0959652619321158.

85. Hengevoss, D., Baumgartner, C., Nisato, G., Energy, C. H.-S., & 2016, undefined. (n.d.). Life Cycle Assessment and eco-efficiency of prospective, flexible, tandem organic photovoltaic module. ElsevierD Hengevoss, C Baumgartner, G Nisato, C HugiSolar Energy, 2016•Elsevier. Retrieved January 10, 2025, from https://www.sciencedirect.com/science/article/pii/S0038092X16303620.

86. Tsang, M. P., Sonnemann, G. W., & Bassani, D. M. (2016). A comparative human health, ecotoxicity, and product environmental assessment on the production of organic and silicon solar cells. Progress in Photovoltaics: Research and Applications, 24(5), 645–655. https://doi.org/10.1002/PIP.2704.

87. Lamnatou, C., Moreno, A., … D. C.-… and S. E., & 2018, undefined. (n.d.). Ethylene tetrafluoroethylene (ETFE) material: Critical issues and applications with emphasis on buildings. ElsevierC Lamnatou, A Moreno, D Chemisana, F Reitsma, F ClariáRenewable and Sustainable Energy Reviews, 2018•Elsevier. https://doi.org/10.1016/j.rser.2017.08.072.

88. Lamnatou, C., Moreno, A., Chemisana, D., Riverola, A., & Solans, A. (2024). Life-cycle assessment of solar façades – The role of ethylene tetrafluoroethylene in building-integrated applications. Solar Energy, 267, 112251. https://doi.org/10.1016/J.SOLENER.2023.112251.

89. Li, Q., Long, L., Li, X., Yang, G., Bian, C., Zhao, B., Chen, X., & Chen, B. M. (2025). Life cycle cost analysis of circular photovoltaic façade in dense urban environment using 3D modeling. Renewable Energy, 238, 121914. https://doi.org/10.1016/J.RENENE.2024.121914.

90. Li, Q., Zhu, L., Sun, Y., Lu, L., Energy, Y. Y.-, & 2020, undefined. (n.d.). Performance prediction of Building Integrated Photovoltaics under no-shading, shading and masking conditions using a multi-physics model. ElsevierQ Li, L Zhu, Y Sun, L Lu, Y YangEnergy, 2020•Elsevier. Retrieved January 10, 2025, from https://www.sciencedirect.com/science/article/pii/S0360544220319022.

91. An, Y., Kim, J., Joo, H., Lee, W., Han, G., Kim, H., Energy, M. K.-R., & 2023, undefined. (n.d.). Experimental performance analysis of photovoltaic systems applied to an positive energy community based on building renovation. ElsevierY An, J Kim, HJ Joo, WJ Lee, G Han, H Kim, MH KimRenewable Energy, 2023•Elsevier. Retrieved January 10, 2025, from https://www.sciencedirect.com/science/article/pii/S0960148123012843.

92. Čurpek, J., Energy, M. Č.-R., & 2020, undefined. (n.d.). Climate response of a BiPV façade system enhanced with latent PCM-based thermal energy storage. ElsevierJ Čurpek, M ČekonRenewable Energy, 2020•Elsevier. Retrieved January 10, 2025, from https://www.sciencedirect.com/science/article/pii/S0960148120300896.

93. Matsuki, N. (2023). The Next Frontier of Solar Energy: Transparent Photovoltaics. ECS Meeting Abstracts, MA2023-02(44), 2170. https://doi.org/10.1149/MA2023-02442170MTGABS.

94. Wu, Z., Zhang, L., Wu, J., Energy, Z. L.-, & 2022, undefined. (n.d.). Experimental and numerical study on the annual performance of semi-transparent photovoltaic glazing in different climate zones. ElsevierZ Wu, L Zhang, J Wu, Z LiuEnergy, 2022•Elsevier. Retrieved January 9, 2025, from https://www.sciencedirect.com/science/article/pii/S0360544221027225.

95. Zhou, H., Energy, H. K.-M. T., & 2023, undefined. (n.d.). Effective redox shuttles for polymer gel electrolytes-based quasi-solid-state dye-sensitized solar cells in outdoor and indoor applications: Comprehensive comparison . ElsevierH Zhou, HK KimMaterials Today Energy, 2023•Elsevier. Retrieved January 9, 2025, https://www.sciencedirect.com/science/article/pii/S2468606923000552.

96. Yang, Y., Stensitzki, T., Sauthof, L., Schmidt, A., Piwowarski, P., Velazquez Escobar, F., Michael, N., Duc Nguyen, A., Szczepek, M., Nikolas Brünig, F., Rüdiger Netz, R., Mroginski, M. A., Adam, S., Bartl, F., Schapiro, I., Hildebrandt, P., Scheerer, P., & Heyne, K. (n.d.). Ultrafast proton-coupled isomerization in the phototransformation of phytochrome. Nature.ComY Yang, T Stensitzki, L Sauthof, A Schmidt, P Piwowarski, F Velazquez Escobar, N MichaelNature Chemistry, 2022•nature.Com. https://doi.org/10.1038/s41557-022-00944-x.

97. Wu, C., Li, R., Wang, Y., Lu, S., Lin, J., ... Y. L.-C., & 2020, undefined. (n.d.). Strong metal– support interactions enable highly transparent Pt–Mo 2 C counter electrodes of bifacial dyesensitized solar cells. Pubs.Rsc.OrgC Wu, R Li, Y Wang, S Lu, J Lin, Y Liu, X ZhangChemical Communications,2020•pubs.Rsc.Org.Retrieved January 9, 2025, from https://pubs.rsc.org/en/content/articlehtml/2020/cc/d0cc03744c.

98. Venkatesan, S., Chen, Y., Chien, C., ... M. T.-J. of I. and, & 2022, undefined. (n.d.). Composite electrolyte pastes for preparing sub-module dye sensitized solar cells. ElsevierS Venkatesan, YY Chen, CY Chien, MH Tsai, H Teng, YL LeeJournal of Industrial and Engineering Chemistry, 2022•Elsevier. Retrieved January 9, 2025, from https://www.sciencedirect.com/science/article/pii/S1226086X21006705.

99. Wong, V. K., Ho, J. K. W., Wong, W. W. H., & So, S. K. (2025). Semi-transparent solar cells: strategies for maximum power output in cities. Energy & Environmental Science. https://doi.org/10.1039/D4EE03757J.

100. Kumar, P., You, S., & Vomiero, A. (2023). Recent Progress in Materials and Device Design for Semitransparent Photovoltaic Technologies. Advanced Energy Materials, 13(39), 2301555. https://doi.org/10.1002/AENM.202301555.

101. Chen, J., Cranton, W., & Fihn, M. (2011). Handbook of visual display technology. https://dl.acm.org/doi/abs/10.5555/2161910.

102. A critical review on semitransparent organic solar cells. (n.d.). ElsevierZ Hu, J Wang, X Ma, J Gao, C Xu, K Yang, Z Wang, J Zhang, F ZhangNano Energy, 2020•Elsevier. Retrieved January 9, 2025, from https://www.sciencedirect.com/science/article/pii/S2211285520309538.

103. Røyset, A., Kolås, T., Buildings, B. J.-E. and, & 2020, undefined.(n.d.). Coloured building-integrated photovoltaics:Influence on energy efficiency. ElsevierA Røyset, T Kolås, BP JelleEnergy and Buildings, 2020•Elsevier. Retrieved January 9, 2025, from https://www.sciencedirect.com/science/article/pii/S0378778819322091.

104. Roy, A., Ghosh, A., Bhandari, S., Selvaraj, P., Sundaram, S., & Mallick, T. K. (2019). Colour comfort evaluation of dye-sensitized solar cell (DSSC) based building-integrated photovoltaic (BIPV) glazing after 2 years of ambient exposure. ACS Publications, A Roy, A Ghosh, S Bhandari, P Selvaraj, S Sundaram, TK MallickThe Journal of Physical Chemistry C, 2019•ACS Publications, 123(39), 23834–23837. https://doi.org/10.1021/acs.jpcc.9b05591.

105. Ahmed, W., & Asif, M. (2020). BIM-based techno-economic assessment of energy retrofitting residential buildings in hot humid climate. Energy and Buildings, 227. https://doi.org/10.1016/J.ENBUILD.2020.110406.

106. Imam, A., Sustainability, Y. A.-T.-, & 2019, undefined. (2020). Techno-economic feasibility assessment of grid-connected PV systems for residential buildings in Saudi Arabia—A case study. Mdpi.ComAA Imam, YA Al-TurkiSustainability, 2019•mdpi.Com, 12(1). https://doi.org/10.3390/su12010262.

107. Lopez-Ruiz, H. G., Blazquez, J., & Vittorio, M. (2020). Assessing residential solar rooftop potential in Saudi Arabia using nighttime satellite images: A study for the city of Riyadh. Energy Policy, 140. https://doi.org/10.1016/J.ENPOL.2020.111399.

108. Mesloub, A., & Ghosh, A. (2020). Daylighting performance of light shelf photovoltaics (LSPV) for office buildings in hot desert-like regions. Applied Sciences (Switzerland), 10(22), 1–24. https://doi.org/10.3390/APP10227959.

109. Sustainability, O. A.-, & 2018, undefined. (2018). Solar and shading potential of different configurations of building-integrated photovoltaics used as shading devices, considering hot climatic conditions. Mdpi.ComOS AsfourSustainability, 2018•mdpi.Com, 10(12). https://doi.org/10.3390/su10124373.

110. Oh, S., Hildreth, A., Oh, S., Energy, A. H.-A. for S., & 2016, undefined. (n.d.). Energy Simulation Using EnergyPlusTM for Building and Process Energy Balance. SpringerSC Oh, AJ Hildreth, SC Oh, AJ Hildreth

,Analytics for Smart Energy Management: Tools and Applications for Sustainable, 2016•Springer. Retrieved January 9, 2025, from https://link.springer.com/chapter/10.1007/978-3319-32729-7_7.

111. Mohsenin, M., & Hu, J. (2015). Assessing daylight performance in atrium buildings by using Climate-Based Daylight Modelling. Solar Energy, 119, 553–560. https://doi.org/10.1016/J.SOLENER.2015.05.011.

112. Matsuki, N. (2023). The Next Frontier of Solar Energy: Transparent Photovoltaics. ECS Meeting Abstracts, MA2023-02(44), 2170. https://doi.org/10.1149/MA2023-02442170MTGABS.

113. Shi, Y., Wang, Y., Lin, J., Li, Y., Guo, X., Jin, C., Wang, Y., & Zhang, X. (2025). Highperformance Cu-based PEO/PVDF-HPF gel polymer electrolyte of semi-transparent dye-sensitized solar cells. Journal of Power Sources, 628, 235876. https://doi.org/10.1016/J.JPOWSOUR.2024.235876.

114. Kwon, H. C., Ma, S., Yun, S. C., Jang, G., Yang, H., & Moon, J. (2020). A nanopillar-structured perovskite-based efficient semitransparent solar module for power-generating window applications. Journal of Materials Chemistry A, 8(3), 1457–1468. https://doi.org/10.1039/C9TA11892F.

115. Rai, M., Yuan, Z., Sadhu, A., Leow, S. W., Etgar, L., Magdassi, S., & Wong, L. H. (2021). Multimodal Approach towards Large Area Fully Semitransparent Perovskite Solar Module. Advanced Energy Materials, 11(45), 2102276. https://doi.org/10.1002/AENM.202102276.

116. Sun, S., Zha, W., Tian, C., Wei, Z., Luo, Q., Ma, C. Q., Liu, W., & Zhu, X. (2023). Solution Processed Semi-Transparent Organic Solar Cells Over 50% Visible Transmittance Enabled by Silver Nanowire Electrode with Sandwich Structure. Advanced Materials, 35(46), 2305092. https://doi.org/10.1002/ADMA.202305092.

117. Li, Y., He, C., Zuo, L., Zhao, F., Zhan, L., Li, X., Xia, R., Yip, H. L., Li, C. Z., Liu, X., & Chen, H. (2021). High-Performance Semi-Transparent Organic Photovoltaic Devices via Improving Absorbing Selectivity. Advanced Energy Materials, 11(11), 2003408. https://doi.org/10.1002/AENM.202003408.

118. Chang, L., Duan, L., Sheng, M., Yuan, J., Yi, H., Zou, Y., & Uddin, A. (2020). Optimising NonPatterned MoO3/Ag/MoO3 Anode for High-Performance Semi-Transparent Organic Solar Cells towards Window Applications. Nanomaterials 2020, Vol. 10, Page 1759, 10(9), 1759. https://doi.org/10.3390/NANO10091759.

119. Nazir, S., Singh, P. K., Rawat, N., Jain, A., Michalska, M., Yahya, M. Z. A., Yusuf, S. N. F., & Diantoro, M. (2025). Polyether (polyethylene oxide) derived carbon electrode material and polymer electrolyte for supercapacitor and dye-sensitised solar cell. Ionics 2025, 1–11. https://doi.org/10.1007/S11581-024-06052-9.

120. Jothi, M. A., Vanitha, D., Bahadur, S. A., & Nallamuthu, N. (2021). Promising biodegradable polymer blend electrolytes based on cornstarch:PVP for electrochemical cell applications. Bulletin of Materials Science, 44(1). https://doi.org/10.1007/S12034-021-02350-4.

121. Jothi, M., Vanitha, D., ... K. S.-I. J. of, & 2022, undefined. (n.d.). Utilisation of corn starch in production of 'eco friendly'polymer electrolytes for proton battery applications. ElsevierMA Jothi, D Vanitha, K Sundaramahalingam, N NallamuthuInternational Journal of Hydrogen Energy, 2022•Elsevier. https://www.sciencedirect.com/science/article/pii/S0360319922028270.

122. Jothi, M. A., Vanitha, D., Sundaramahalingam, K., & Nallamuthu, N. (2022). Utilisation of corn starch in production of 'eco friendly' polymer electrolytes for proton battery applications. International Journal of Hydrogen Energy, 47(67), 28763–28772. https://doi.org/10.1016/J.IJHYDENE.2022.06.192.

123. Konwar, S., Kumar, S., Mohamad, A. A., Jain, A., Michalska, M., Punetha, V. D., Yahya, M. Z. A., Strzałkowski, K., Singh, D., Diantoro, M., Chowdhury, F. I., & Singh, P. K. (2025). Ionic liquid (1Ethyl-3-methylimidazolium tricyanomethanide) incorporated corn starch polymer electrolyte for solar cell and supercapacitor application. Chemical Physics Impact, 10, 100780. https://doi.org/10.1016/J.CHPHI.2024.100780.

124. Gorjian, S., Bousi, E., Özdemir, Ö. E., Trommsdorff, M., Kumar, N. M., Anand, A., Kant, K., & Chopra, S. S. (2022). Progress and challenges of crop production and electricity generation in agrivoltaic systems using semi-transparent photovoltaic technology. Renewable and Sustainable Energy Reviews, 158, 112126. https://doi.org/10.1016/J.RSER.2022.112126.

125. Barichello, J., Vesce, L., Mariani, P., Leonardi, E., Braglia, R., di Carlo, A., Canini, A., & Reale, A. (2021). Stable Semi-

Transparent Dye-Sensitized Solar Modules and Panels for Greenhouse Application. Energies 2021, Vol. 14, Page 6393, 14(19), 6393. https://doi.org/10.3390/EN14196393.

126. Jinnai, S., Oi, A., Seo, T., Moriyama, T., Terashima, M., Suzuki, M., Nakayama, K. I., Watanabe, Y., & Ie, Y. (2023). Green-Light Wavelength-Selective Organic Solar Cells Based on Poly(3hexylthiophene) and Naphthobisthiadiazole-Containing Acceptors toward Agrivoltaics. ACS Sustainable Chemistry and Engineering, 11(4), 1548–1556. https://doi.org/10.1021/ACSSUSCHEMENG.2C06426/SUPPL_FILE/SC2C06426_SI_001.PDF.

127. Wang, Y., Wang, G., Xing, Y., ... M. A.-M. C., & 2021, Top and bottom electrode optimization enabled high-performance flexible and semi-transparent organic solar cells .Pubs.Rsc.OrgY Wang, G Wang, Y Xing, MA Adil, WA Memon, Y Chang, L Liu, C Yang, M Zhang, D LiMaterials Chemistry Frontiers, 2021•pubs.Rsc.Org. Retrieved January 10, 2025, from https://pubs.rsc.org/en/content/articlehtml/2021/qm/d1qm00151e.

128. Xue, Z., Yu, R., Zhu, M., Wu, Y., He, Y., Gao, X., Letters, Y. T.-M., & 2021 - ,undefined. (n.d.). Effectively enhancing the open-circuit voltage via chlorinated substitution in DPP-based polymer donor for polymer solar cells .ElsevierZ Xue, R Yu, M Zhu, Y Wu, Y He, X Gao, Y TaoMaterials Letters, 2021•Elsevier. Retrieved January 10, 2025, from https://www.sciencedirect.com/science/article/pii/S0167577X21009198.

129. Lee, J., Han, A. R., Hong, J., Seo, J. H., Oh, J. H., & Yang, C. (2012). Inversion of dominant polarity in ambipolar polydiketopyrrolopyrrole with thermally removable groups. Advanced Functional Materials, 22(19), 4128–4138. https://doi.org/10.1002/ADFM.201200940.

130. Rasool, S., Hoang, Q., Vu, D. van, ... C. S.-J. of E., & 2022, undefined. (n.d.). High-efficiency single and tandem fullerene solar cells with asymmetric monofluorinated diketopyrrolopyrrolebased polymer. Elsevier. Retrieved January 10, 2025, from https://www.sciencedirect.com/science/article/pii/S2095495621002448.

131. Park, B., Bae, H., Ha, J. W., Lee, C., Lee, J., Heo, Y., Kim, B. S., Yoon, S. C., Choi, H., & Ko, S. J. (2023). Synthesis of a halogenated low bandgap polymeric donor for semi-transparent and near-infrared organic solar cells. Organic Electronics, 113, 106717. https://doi.org/10.1016/J.ORGEL.2022.106717.

132. Rahman, M. Y. A., Salleh, M. M., Talib, I. A., & Yahaya, M. (2004). Effect of ionic conductivity of a PVC–LiClO4 based solid polymeric electrolyte on the performance of solar cells of ITO/TiO2/PVC–LiClO4/graphite. Journal of Power Sources, 133(2), 293–297. https://doi.org/10.1016/J.JPOWSOUR.2004.03.029.

133. Ileperuma, O. A., Asoka Kumara, G. R., Yang, H.-S., & Murakami, K. (2011.). Quasi-solid electrolyte based on polyacrylonitrile for dye-sensitized solar cells. Elsevier. Retrieved January 14, 2025, from https://www.sciencedirect.com/science/article/pii/S1010603010004508.

134. Balamurugan, S., Ganesan, S., Kamaraj, S., Mathew, V., Kim, J., Arumugam, N., & Almansour, A. I. (2022). Effect of poly (ethylene glycol) gel polymer electrolyte consist of novel heteroleptic cobalt redox shuttle and pyridine based organic additive on performance of dye sensitized solar cells. Optical Materials, 125, 112082. https://doi.org/10.1016/J.OPTMAT.2022.112082.

135. Wu, J., Lan, Z., Wang, D., Hao, S., Lin, J., Huang, Y., Yin, S., & Sato, T. (2006). Gel polymer electrolyte based on poly(acrylonitrile-co-styrene) and a novel organic iodide salt for quasi-solid state dye-sensitized solar cell. Electrochimica Acta, 51(20), 4243–4249.https://doi.org/10.1016/J.ELECTACTA.2005.11.047.

136. Kim, D. W., Jeong, Y. B., Kim, S. H., Lee, D. Y., & Song, J. S. (2005). Photovoltaic performance of dye-sensitized solar cell assembled with gel polymer electrolyte. Journal of Power Sources, 149(1–2), 112–116. https://doi.org/10.1016/J.JPOWSOUR.2005.01.058.

137. Abisharani, J. M., Balamurugan, S., Thomas, A., Devikala, S., Arthanareeswari, M., Ganesan, S., & Prakash, M. (2021). Incorporation of organic additives with electron rich donors (N, O, S) in gelatin gel polymer electrolyte for dye sensitized solar cells. Solar Energy, 218, 552–562. https://doi.org/10.1016/J.SOLENER.2021.03.007.

138. Bettucci, O., Saavedra Becerril, V., Bandara, T. M. W. J., Furlani, M., Abrahamsson, M., Mellander, B. E., & Zani, L. (2018). Organic dye-sensitized solar cells containing alkaline iodidebased gel polymer electrolytes: influence of cation size. Physical Chemistry Chemical Physics, 20(2), 1276–1285. https://doi.org/10.1039/C7CP07544H.

139. Shen, S. Y., Dong, R. X., Shih, P. T., Ramamurthy, V., Lin, J. J., & Ho, K. C. (2014). Novel polymer gel electrolyte with organic solvents for quasi-solid-state dye-sensitized

solar cells. ACS Applied Materials and Interfaces, 6(21), 18489–18496. https://doi.org/10.1021/AM505394V/SUPPL_FILE/AM505394V_SI_001.PDF.

140. Shi, J., Wang, L., Liang, Y., Peng, S., ... F. C.-T. J. of, & 2010, undefined. (2010). All-Solid-State Dye-Sensitized Solar Cells with Alkyloxy-Imidazolium Iodide Ionic Polymer/SiO2 Nanocomposite Electrolyte and Triphenylamine-Based Organic Dyes. ACS PublicationsJ Shi, L Wang, Y Liang, S Peng, F Cheng, J ChenThe Journal of Physical Chemistry C, 2010•ACS Publications, 114(14), 6814–6821. https://doi.org/10.1021/jp100029r.

141. Chang, H., Wu, H., Chen, T., Huang, K., ... C. J.-J. of A. and, & 2010, undefined. (n.d.). Dyesensitised solar cell using natural dyes extracted from spinach and ipomoea. ElsevierH Chang, HM Wu, TL Chen, KD Huang, CS Jwo, YJ LoJournal of Alloys and Compounds, 2010•Elsevier. https://www.sciencedirect.com/science/article/pii/S0925838809020337.

142. Yuliarto, B., Septina, W., Fuadi, K., Fanani, F., Muliani, L., & Suib, S. (2010). Synthesis of Nanoporous TiO2 and Its Potential Applicability for Dye-Sensitized Solar Cell Using Antocyanine Black Rice. Wiley Online LibraryB Yuliarto, W Septina, K Fuadi, F Fanani, L Muliani, NugrahaAdvances in Materials Science and Engineering, 2010•Wiley Online Library, 2010. https://doi.org/10.1155/2010/789541.

143. Zhou, H., Wu, L., Gao, Y., & Ma, T. (2011). Dye-sensitised solar cells using 20 natural dyes as sensitisers. Journal of Photochemistry and Photobiology A: Chemistry, 219(2–3),188–194. https://doi.org/10.1016/J.JPHOTOCHEM.2011.02.008.

144. Ruhane, T. A., Islam, M. T., Rahaman, M. S., Bhuiyan, M. M. H., Islam, J. M. M., Newaz, M. K., Khan, K. A., & Khan, M. A. (2017). Photo current enhancement of natural dye sensitized solar cell by optimizing dye extraction and its loading period. Optik, 149, 174–183. https://doi.org/10.1016/J.IJLEO.2017.09.024.

145. Noor, M. M., Buraidah, M. H., Careem, M. A., Majid, S. R., & Arof, A. K. (2014). An optimized poly (vinylidene fluoride-hexafluoropropylene)–NaIgel polymer electrolyte and its application in natural dye sensitised solar cells. Electrochimica Acta, 121, 159–167. https://doi.org/10.1016/J.ELECTACTA.2013.12.136.

146. Quan, J., Zhou, D., Wan, W., Wang, F., Hu, L., Hu, B., Tong, Y., Wang, J., Lv, R., Li, Z., Wu, F., & Chen, L. (2024). Intramolecular Lock Conjugated Polymer Electrolytes as the Cathode Interfacial Layer for Nonfullerene Organic Solar Cells. ACS Sustainable Chemistry and Engineering, 12(9), 3851–3862. https://doi.org/10.1021/ACSSUSCHEMENG.4C00188/SUPPL_FILE/SC4C00188_SI_001.PDF.

147. Subramanian, A., Murugapoopathi, S., & Amesho, K. T. T. (2024). Enhancing the Performance of Nanocrystalline TiO2 Dye-Sensitized Solar Cells with Phenothiazine-Doped Blended Solid Polymer Electrolyte. Electrocatalysis, 15(2–3), 226–238. https://doi.org/10.1007/S12678-02400867-W/METRICS.

148. Patni, N., & Pillai, S. G. (2025). Improvement in the performance of indium-free dye-sensitised solar cells by the use of polyaniline composite. Materials Chemistry and Physics, 329, 130108. https://doi.org/10.1016/J.MATCHEMPHYS.2024.130108.

149. Zakariya'u, I., Rawat, S., Kathuria, S., Ngulezhu, T., Song, S., Yahya, M. Z. A., Savilov, S. v., Polu, A. R., Singh, R. C., & Singh, P. K. (2024). Efficient, stable dye-sensitised solar cell using ionic liquid–solid polymer electrolyte. Journal of Materials Science: Materials in Electronics, 35(23), 1–9. https://doi.org/10.1007/S10854-024-13301-0/METRICS.

150. O'Regan, B., Lenzmann, F., Muis, R., & Wienke, J. (2002). A solid-state dye-sensitised solar cell fabricated with pressure-treated P25-TiO2 and CuSCN: Analysis of pore filling and IV characteristics. Chemistry of Materials, 14(12), 5023–5029. https://doi.org/10.1021/cm020572d.

151. Wang, P., Zakeeruddin, S. M., Moser, J. E., Nazeeruddin, M. K., Sekiguchi, T., & Grätzel, M. (2003). A stable quasi-solid-state dye-sensitized solar cell with an amphiphilic ruthenium sensitizer and polymer gel electrolyte. Nature Materials, 2(6), 402–407. https://doi.org/10.1038/nmat904.

152. Wang, P.; Zakeeruddin, S.M.; Comte, P.; Charvet, R.; Humphry-Baker, A.R.; Grätzel, M. (2003). Enhance the Performance of Dye-Sensitised Solar Cells by Co-grafting Amphiphilic Sensitiser and Hexadecylmalonic Acid on TiO2 Nanocrystals. J. Phys. Chem. B 107, 14336–14341.

153. Cheng, C.; Wan, C.; Wang, Y. (2004).Preparation of porous, chemically cross-linked, PVdF-based gel polymer electrolytes for rechargeable lithium batteries. J. Power Source, 134, 202–210. https://doi.org/10.1016/j.jpowsour.2004.03.037.

154. Nujud Badawi, M., Bhatia, M., Ramesh, S., Ramesh, K., Kuniyil, M., Shaik, M. R., Khan, M., Shaik, B., & Adil, S. F. (2023). SelfHealing, Flexible and Smart 3D Hydrogel Electrolytes Based on Alginate/PEDOT:PSS for Supercapacitor Applications. Polymers 2023, Vol. 15, Page 571, 15(3), 571. https://doi.org/10.3390/POLYM15030571.

155. O'Regan, B., Grätzel, M.(1991). A low-cost, high-efficiency solar cell based on dye-sensitized colloidal TiO2 films. Nature 353, 737–740. https://doi.org/10.1038/353737a0.

156. Nujud Badawi, M, Bhatia, M., Ramesh, S., Ramesh, K., Khan, M., & Adil, S. F. (2023). Enhancement of the Performance Properties of Pure Cotton Fabric by Incorporating Conducting Polymer (PEDOT:PSS) for Flexible and Foldable Electrochemical Applications. Journal of Electronic Materials 2023, 1–15. https://doi.org/10.1007/S11664-022-10170-3.